



Multiplicity fluctuations and Negative binomial distributions

Tomoaki Nakamura (RIKEN)
for the PHENIX collaboration

Multiplicity distributions are referred to...

- **Hadron production mechanism**

- Particles in jet fragmentation

[I.M. Dremin, J.W. Gary: Phys. Rept. 349, 301]

- **Hadronization, Space-time evolution of QCD matter**

- Relation with Bose-Einstein correlation

[E802 Collaboration: Phys. Rev. C56, 1544]

- **Critical behavior at the QCD phase transition**

- Long-range correlation, Factorial moment, Intermittency

[E.A. De Wolf, I.M. Dremin, W. Kittel: Phys. Rept. 270, 1]

- Isothermal compressibility

[PHENIX Collaboration: Phys. Rev. C78, 044902]

- Density correlation / Susceptibility

[PHENIX Collaboration: Phys. Rev. C76, 034903]

- **Critical point search in QCD phase diagram**

- Energy/Collision species scan at RHIC, SPS, GSI

[NA49 Collaboration: arXiv:0912.4198]

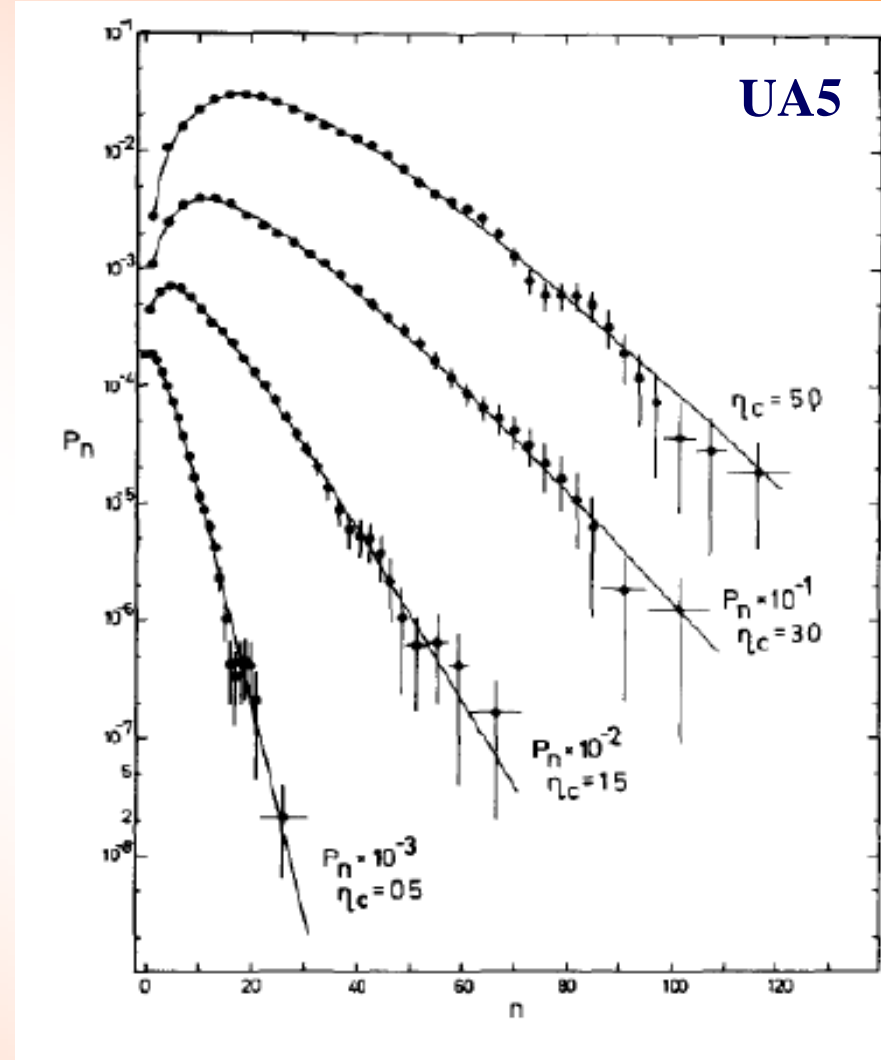
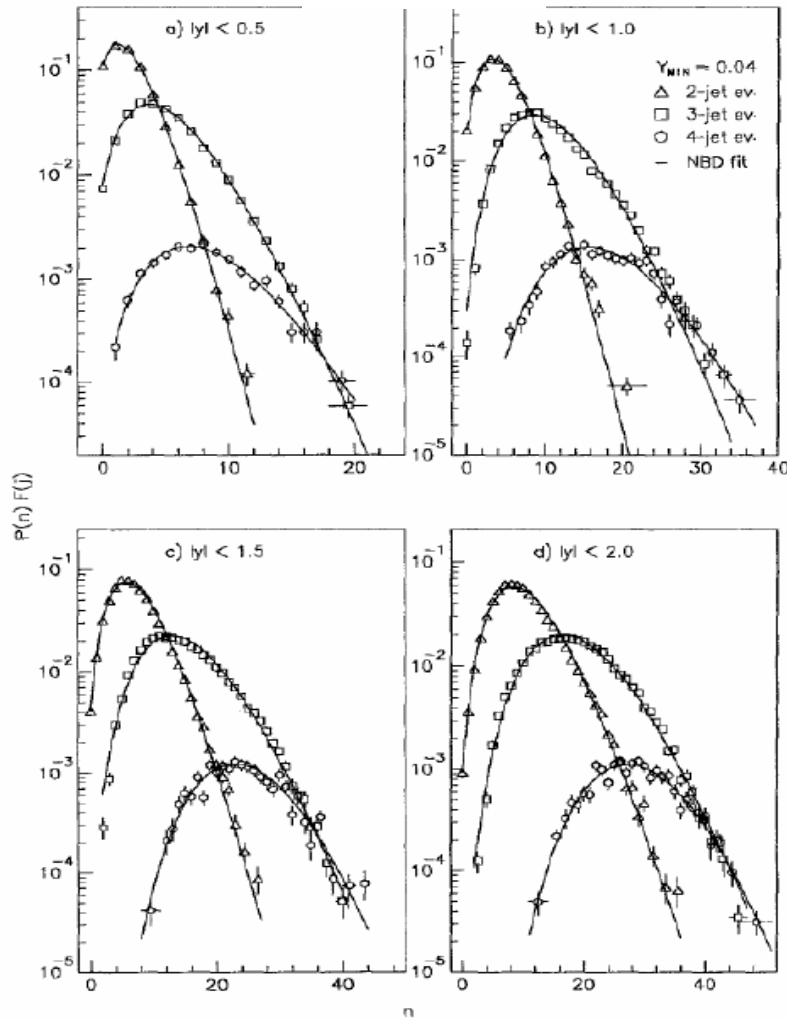
- **CGC and Glasma**

- Is it accessible at LHC?

[F. Gelis, T. Lappi, L. McLerran: Nucl. Phys. A828, 149]

Multiplicity distributions in high energy collisions

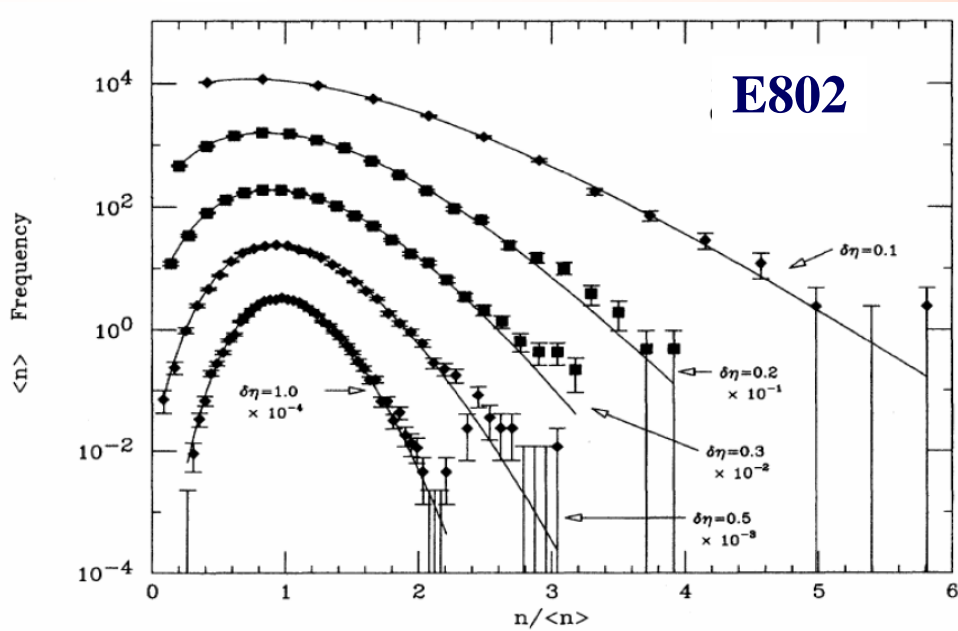
DELPHI



DELPHI: hadronic Z^0 decay, Z. Phys. C56, 63

UA5: p+pbar 540GeV, Phys. Lett. B160, 193

Negative binomial distribution (NBD)



E802: O+Cu 14.6A GeV/c, Phys. Rev. C52, 2663

Poisson distribution ($k = \infty$)

$$P(n) = e^{-\mu} \mu^n / \Gamma(n-1)$$

Negative binomial distribution

$$P(n) = \frac{\Gamma(n+k)}{\Gamma(n+1)\Gamma(k)} \frac{(\mu/k)^n}{(1+\mu/k)^{n+k}}$$

$$\frac{\sigma^2}{\mu^2} = \frac{1}{\mu} + \frac{1}{k} \quad \mu \equiv \langle n \rangle$$

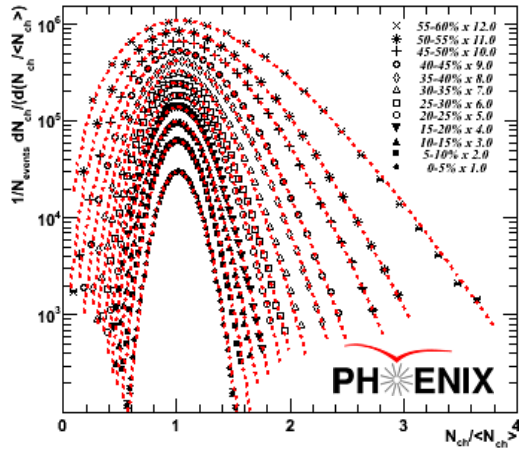
Bose-Einstein distribution ($k = 1$)

$$P(n) = \mu^n / (1+\mu)^{n+1}$$

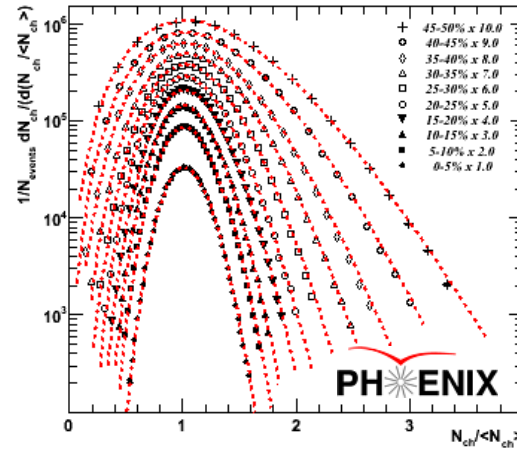
μ : mean of the distribution
 k^{-1} : deviation from Poissonian width
 k : multiplicity of B. E. emission source

NBD in Au+Au, Cu+Cu at RHIC energy

200 GeV Au+Au

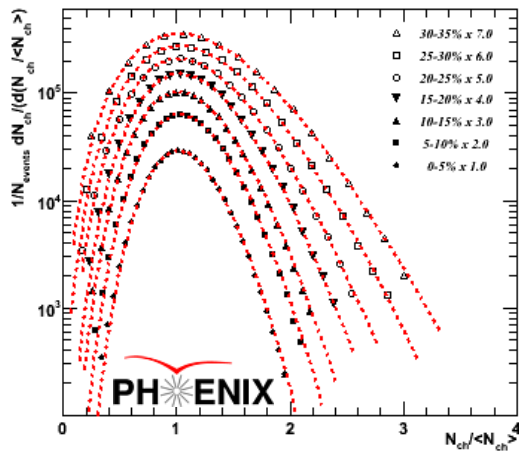


62.4 GeV Au+Au

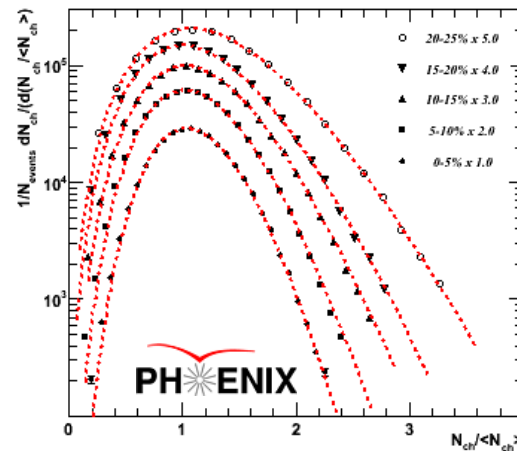


Red lines represent the NBD fits. Multiplicity distributions measured for $0.2 < p_T < 2.0$ GeV/c.

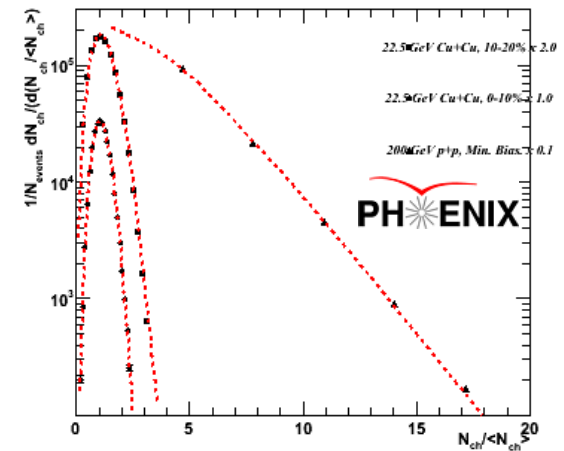
200 GeV Cu+Cu



62.4 GeV Cu+Cu



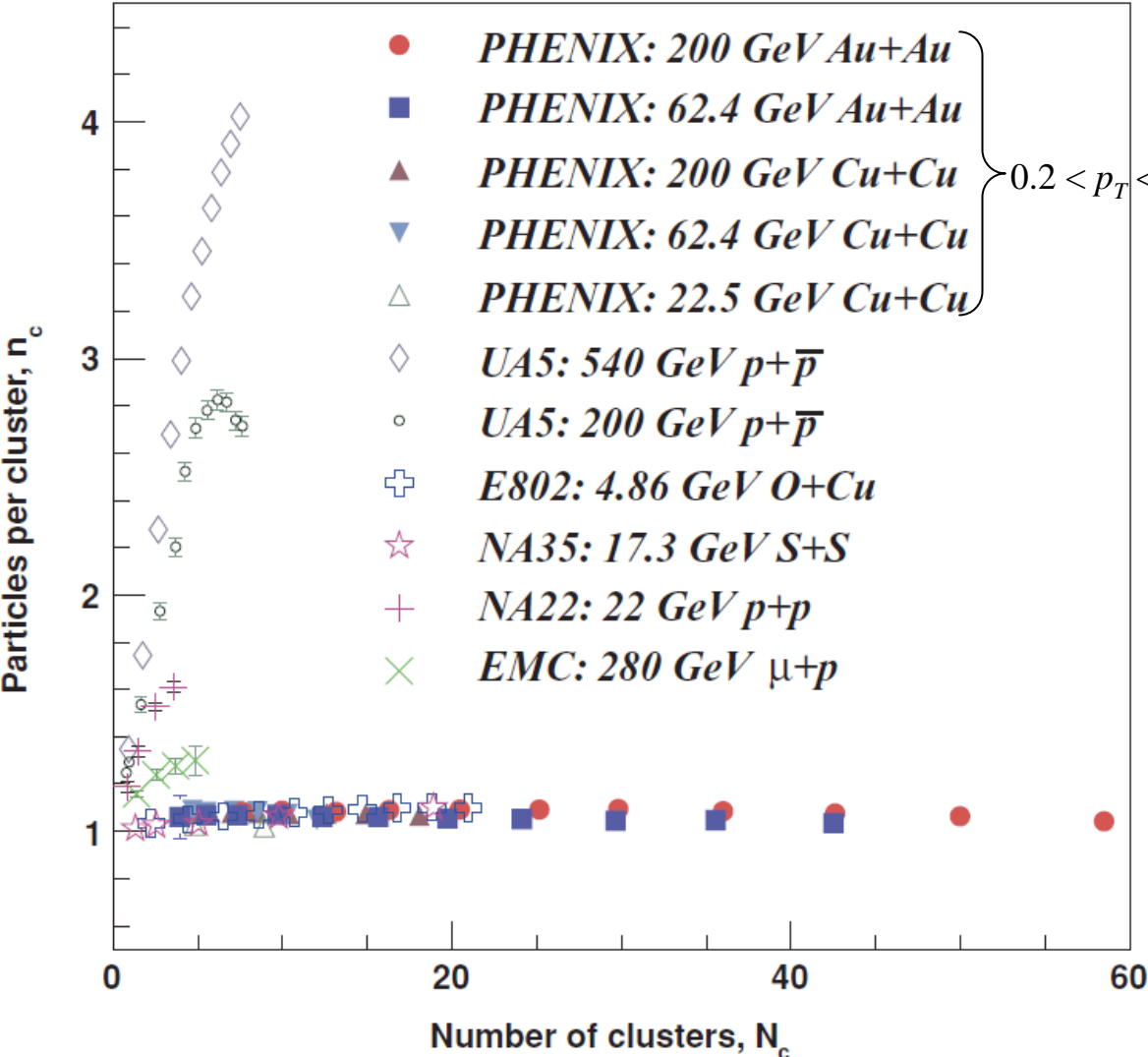
22.5 GeV Cu+Cu



200 GeV p+p

Clan model varying collision energy

A. Giovannini et al., Z. Phys. C30, 391



Hadron production is modeled as independent emission of a number of hadron clusters, N_c , each with a mean number of hadrons, n_c . These parameters can be related to the NBD parameters:

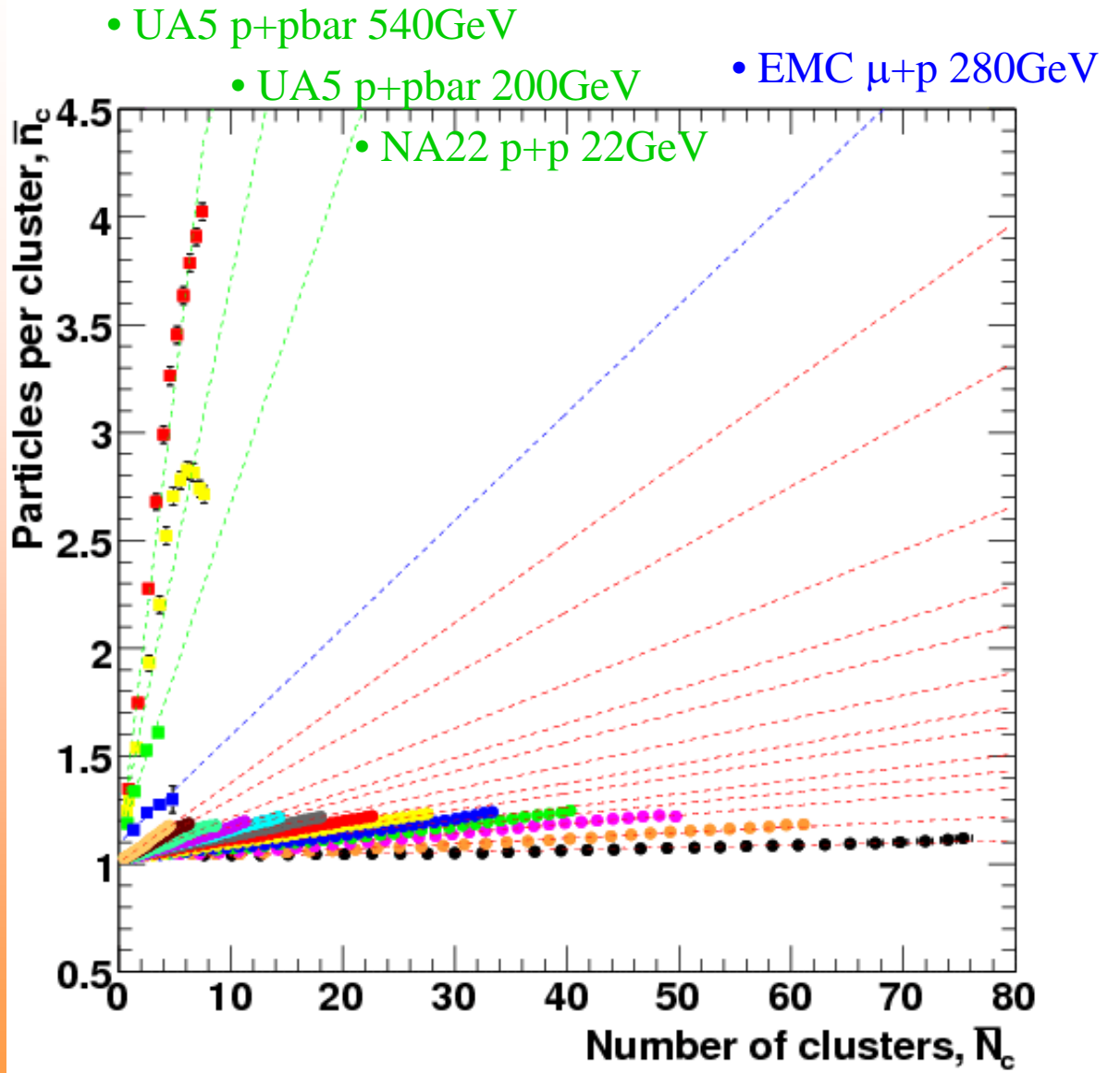
$$\bar{N}_c = k \ln(1 + \mu / k)$$

$$\bar{n}_c = (\mu / k) / \ln(1 + \mu / k)$$

A+A collisions exhibit weak clustering characteristics, independent of collision energy.

PHENIX: Phys. Rev. C78, 044902

Clan model varying pseudo rapidity interval



PHENIX Au+Au 200GeV
($p_T > 0.1$ GeV)

- Centrality 60-65%
- Centrality 55-60%
- Centrality 50-55%
- Centrality 45-50%
- Centrality 40-45%
- Centrality 35-40%
- Centrality 30-35%
- Centrality 25-30%
- Centrality 20-25%
- Centrality 15-20%
- Centrality 10-15%
- Centrality 5-10%
- Centrality 0-5%

Data points in
[Phys. Rev. C76, 034903](#)

Relations with thermodynamic quantities

Prior condition

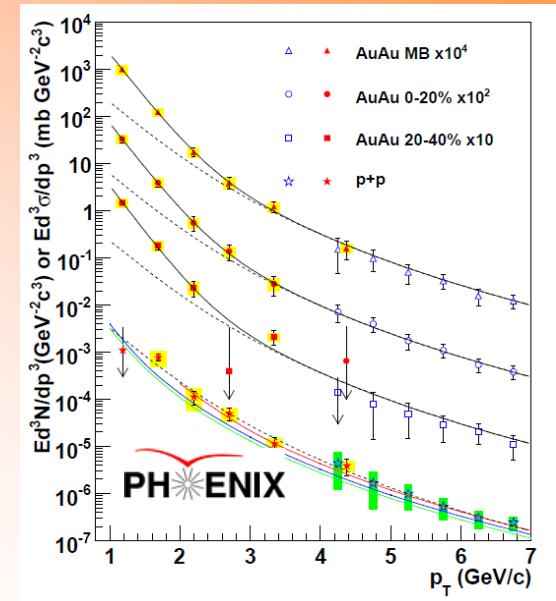
- Thermal photon excess
→ **Lower bound of initial temperature**

Searching for critical behavior

- Mean p_T fluctuation
→ **Heat capacity (specific heat)**

- Multiplicity fluctuation
→ **Compressibility**

- Multiplicity fluctuation with respect to rapidity intervals
→ **Density correlation length**

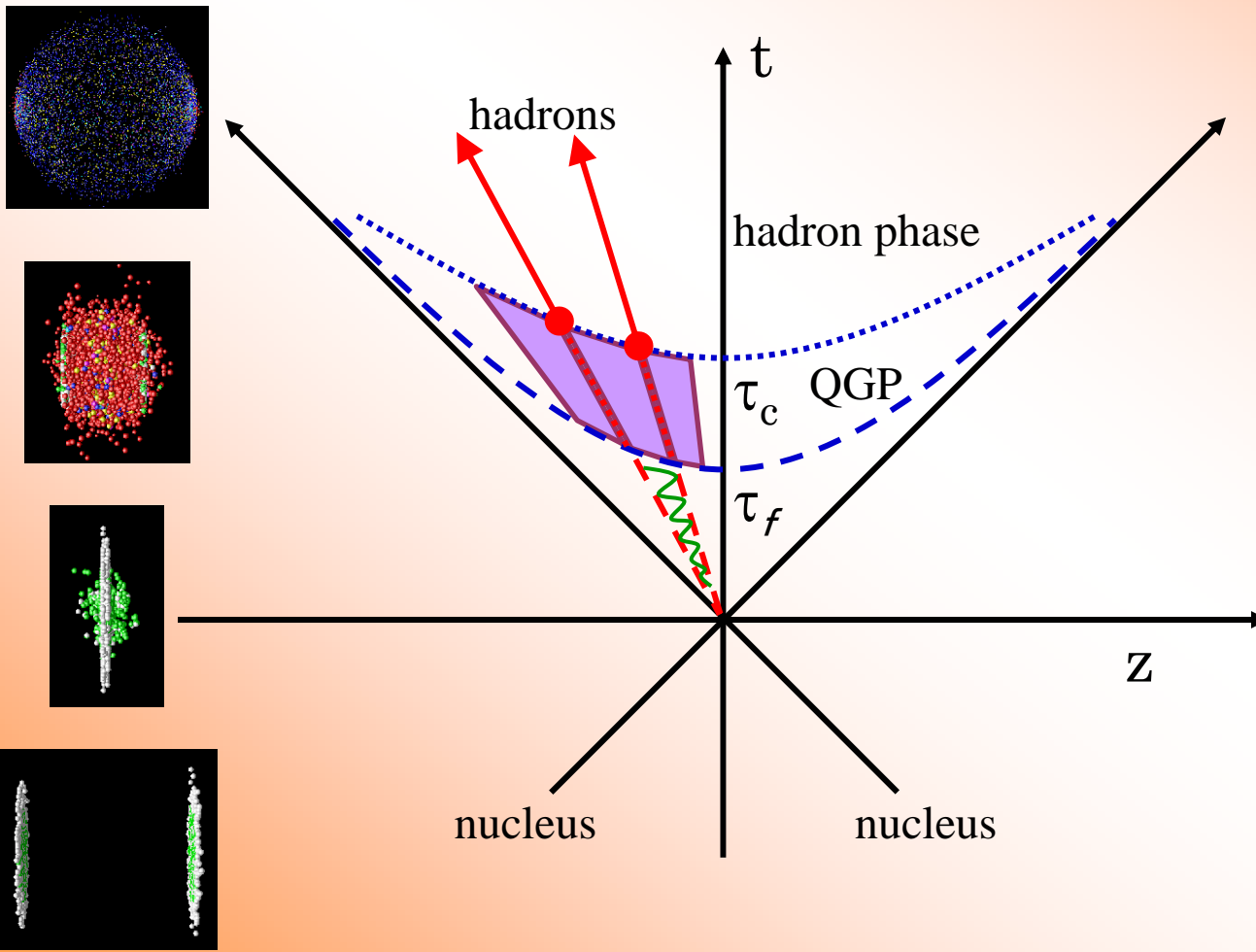


$$\sum_{p_T}, \quad C_V \propto \left(\frac{T - T_c}{T_c} \right)^{-\alpha}$$

$$\frac{\sigma^2}{\mu} = k_B T \left(\frac{\mu}{V} \right) k_T, \quad k_T \propto \left(\frac{T - T_c}{T_c} \right)^{-\gamma}$$

$$\phi(r) = \rho(r) - \langle \rho \rangle, \quad \xi(T) \propto \left(\frac{T - T_c}{T_c} \right)^{-\nu}$$

Density correlation



A common proper time frame should be introduced as shown in the figure for each hydrodynamical sub volume element in this study for the purpose of the application.

Therefore, the differential length dz between the neighboring hydrodynamical volume elements at the common proper time

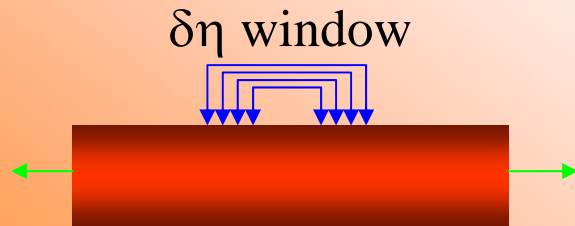
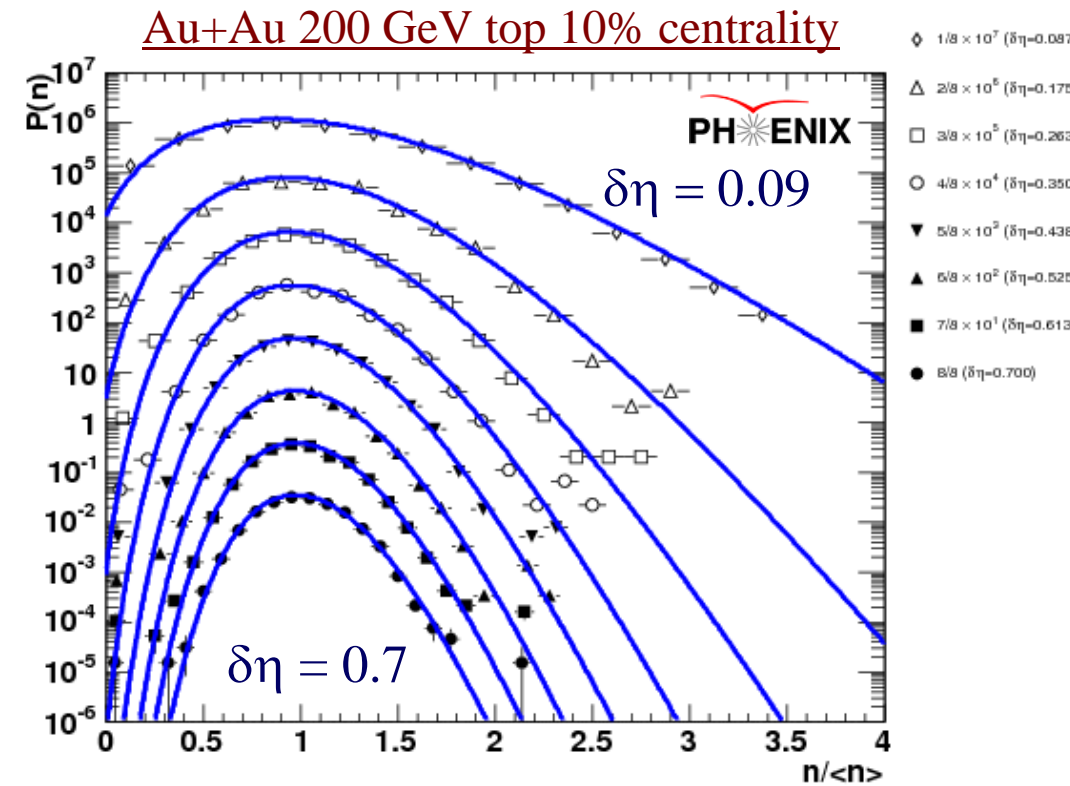
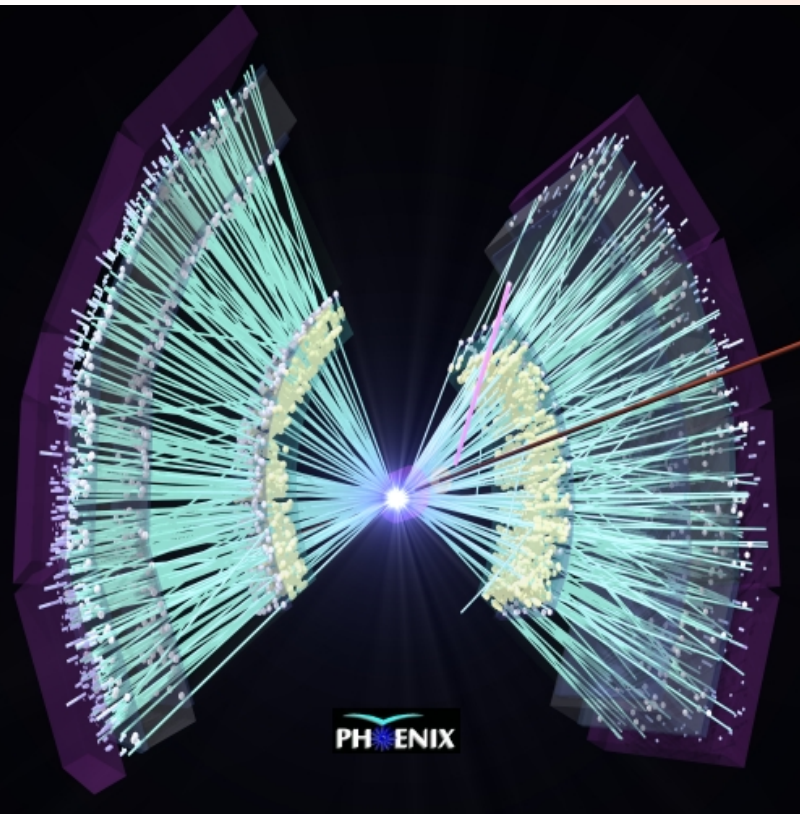
$$\tau = \sqrt{t^2 - z^2}$$

is expressed as

$$dz = \tau \cdot \cosh(y) dy$$

where y is rapidity.

Multiplicity distribution



The distributions are shown as a function of the number of tracks n normalized to the mean multiplicity $\langle n \rangle$ in each $\delta\eta$ window. The solid curves are fit results with NBD only for the demonstration purpose. The fit accuracy corresponds to typically 80% confidence level.

Correlation function

1D Correlation function by Ornstein-Zernike formula

$$\frac{C_2(\eta_1, \eta_2)}{\bar{\rho}_1^2} = \alpha e^{-\delta\eta/\xi} + \beta$$

α : correlation strength

ξ : correlation length

β : rapidity independent correlation

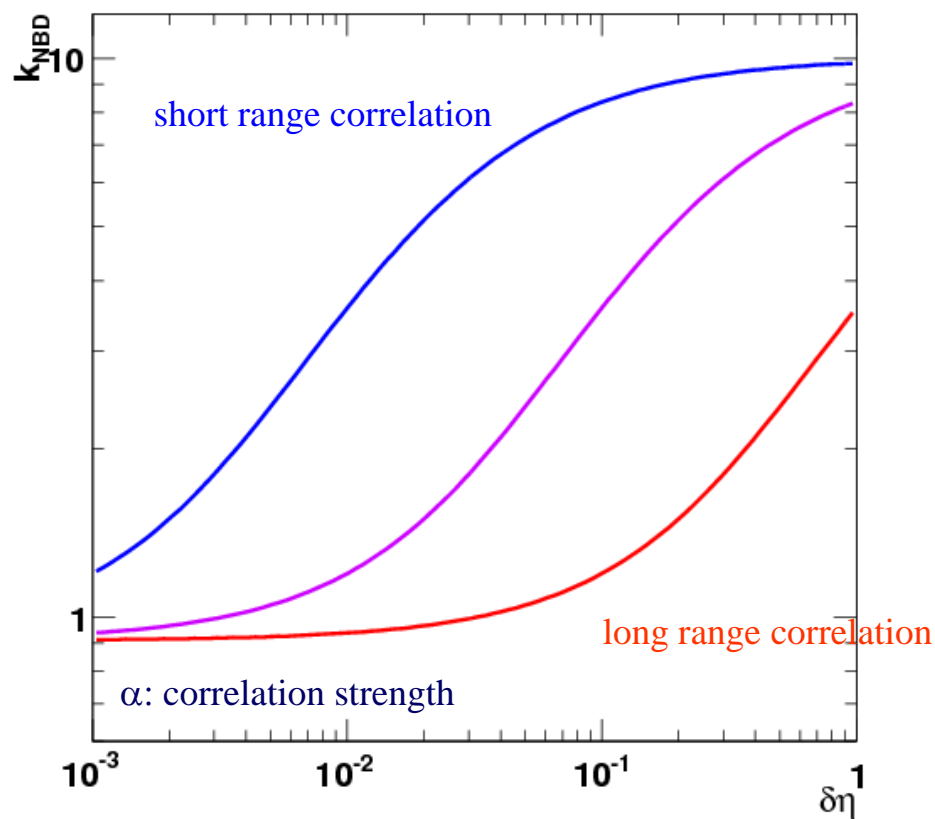
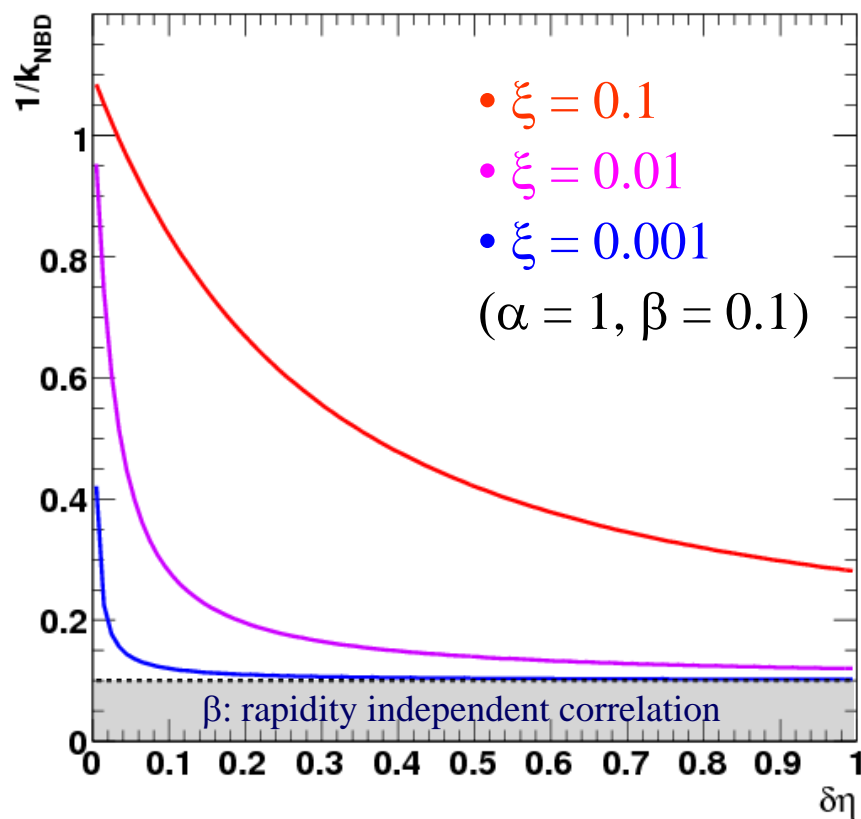
Relation between NBD k and correlation function

$$k^{-1}(\delta\eta) = F_2 - 1 = \frac{\int_0^{\delta\eta} \int_0^{\delta\eta} C_2(\eta_1, \eta_2) d\eta_1 d\eta_2}{\delta\eta^2 \bar{\rho}_1^2}$$

$$k^{-1}(\delta\eta) = \frac{2\alpha\xi^2 (\delta\eta/\xi - 1 + e^{-\delta\eta/\xi})}{\delta\eta^2} + \beta$$

Function shape of NBD k vs. $\delta\eta$

$$k^{-1}(\delta\eta) = F_2 - 1 = \frac{\int_0^{\delta\eta} \int_0^{\delta\eta} C_2(\eta_1, \eta_2) d\eta_1 d\eta_2}{\delta\eta^2 \bar{\rho}_1^2} = \frac{2\alpha\xi^2 (\delta\eta/\xi - 1 + e^{-\delta\eta/\xi})}{\delta\eta^2} + \beta$$



Extraction of the density correlations

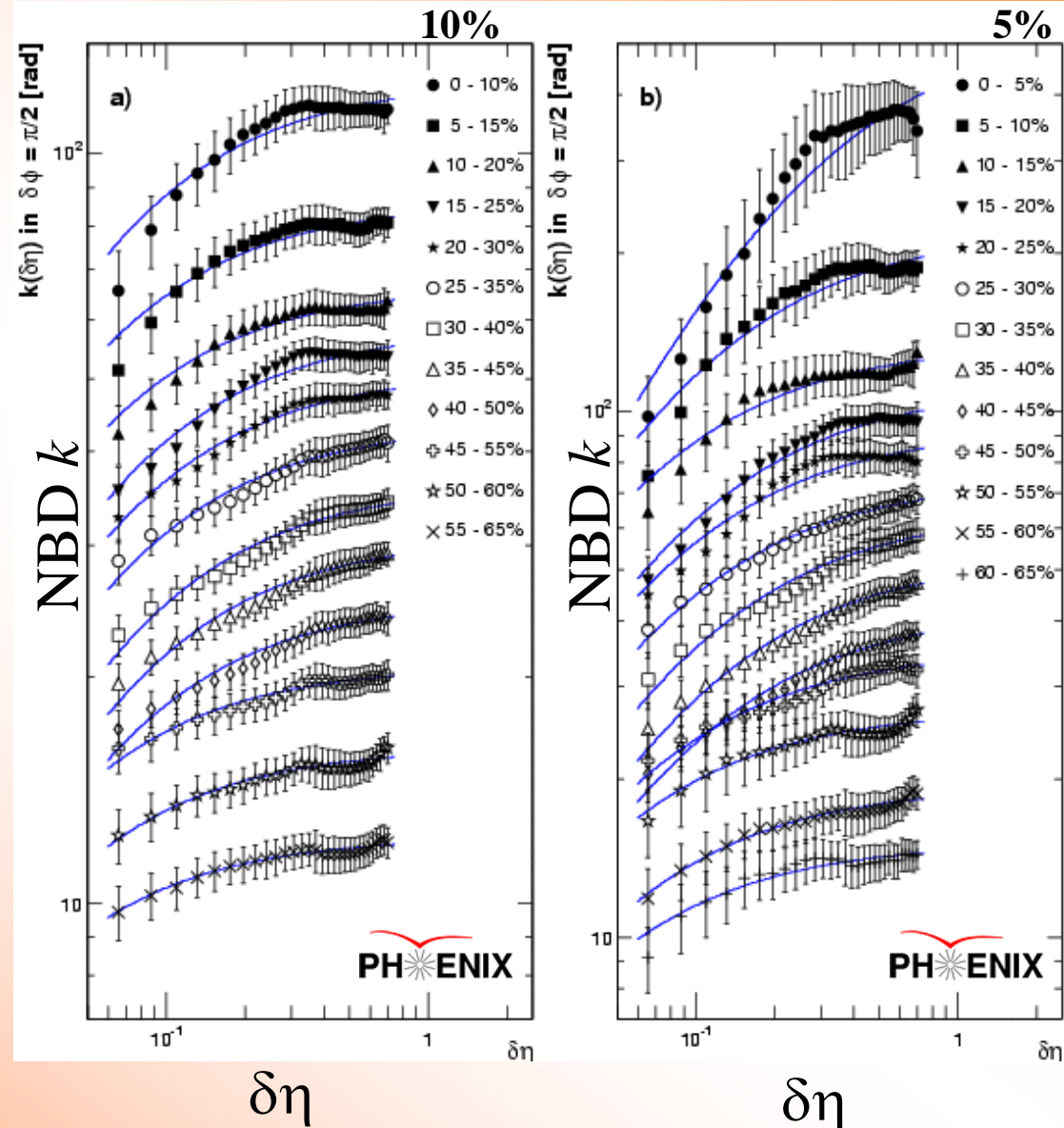
Au+Au 200 GeV

Figure show corrected NBD k as a function of pseudorapidity window size with 10% and 5% centrality bin width, respectively.

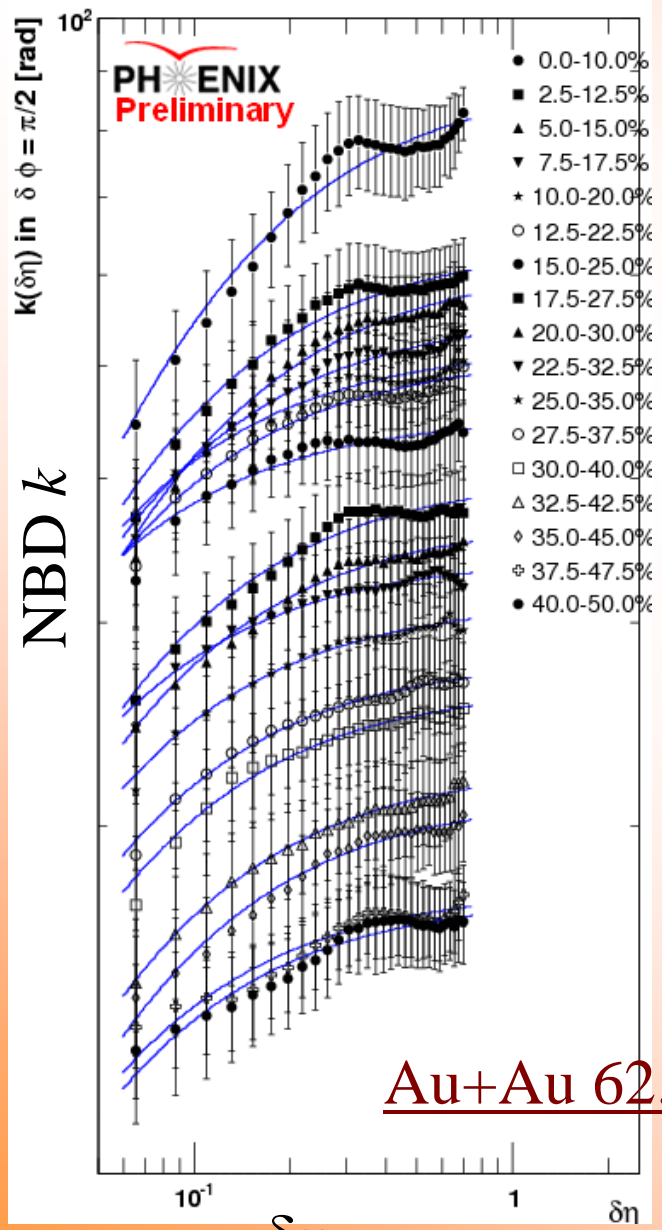
Since the upper limit of ξ is small enough compared to the fitting region of $\delta\eta$, the integrated correlation function can be approximated as follows.

$$k(\delta\eta) = \frac{1}{2\alpha\xi / \delta\eta + \beta} \quad (\xi \ll \delta\eta)$$

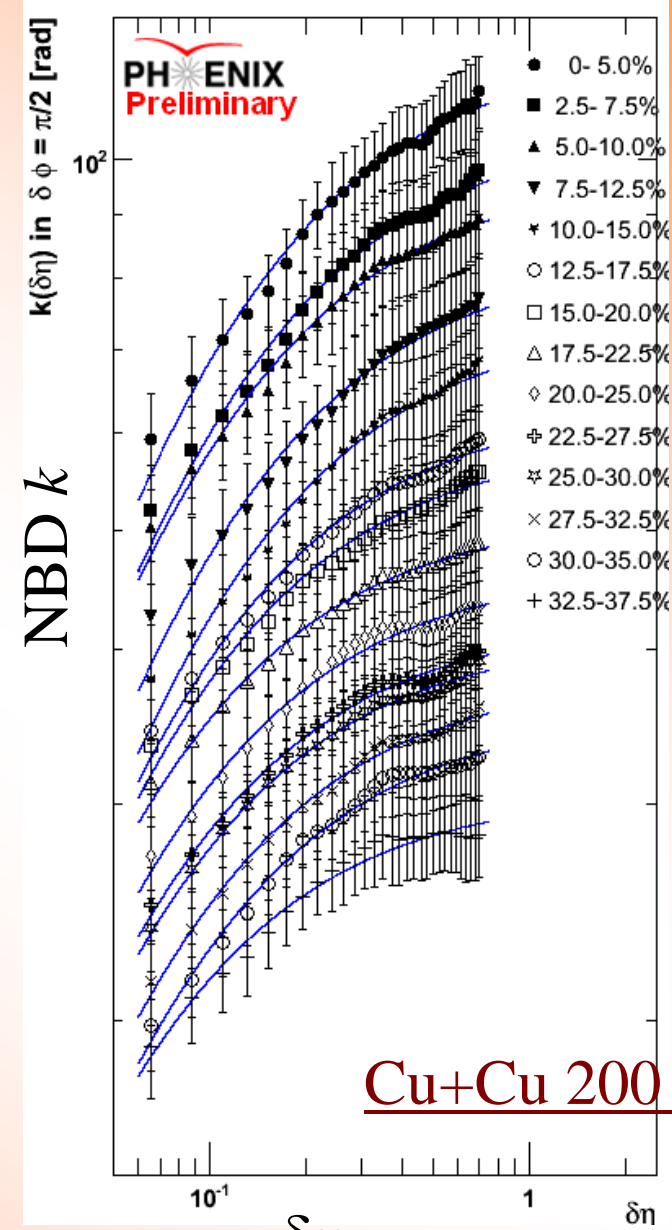
The solid lines in the figure indicate the fit results based on the equation. (99% confidence level)



System and energy dependence

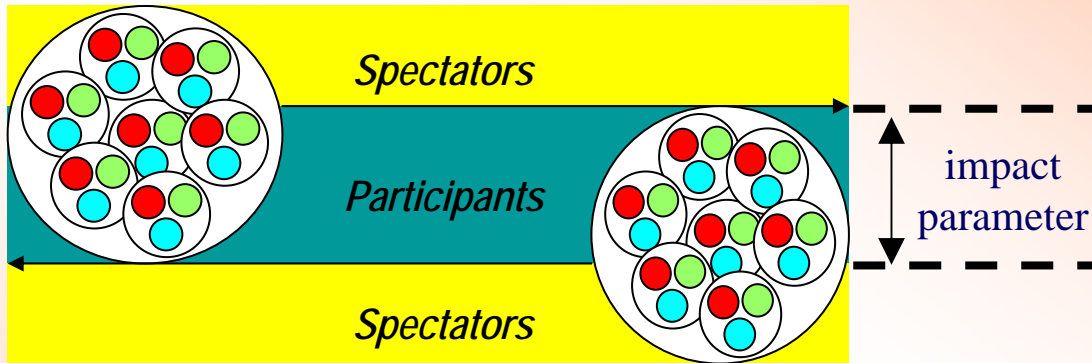


Au+Au 62.4 GeV

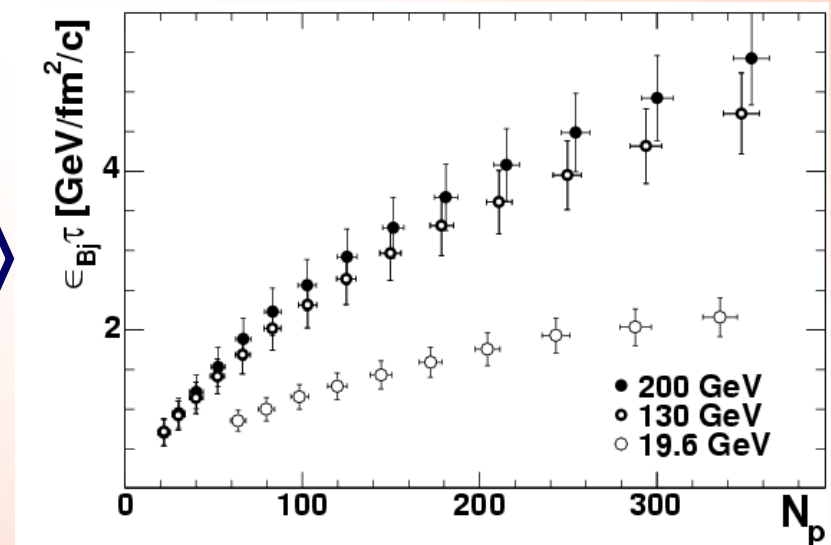
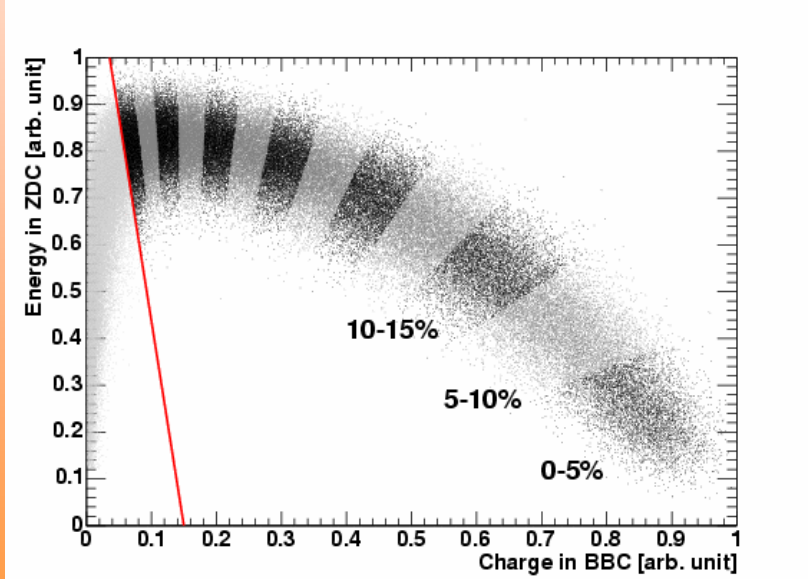


Cu+Cu 200 GeV

Bjorken energy density and Collision centrality



The energy density is more meaningful rather than the total energy, because the particle productions depend not only on the total energy but also on the system size.



Collision centrality classification

Bjorken energy density

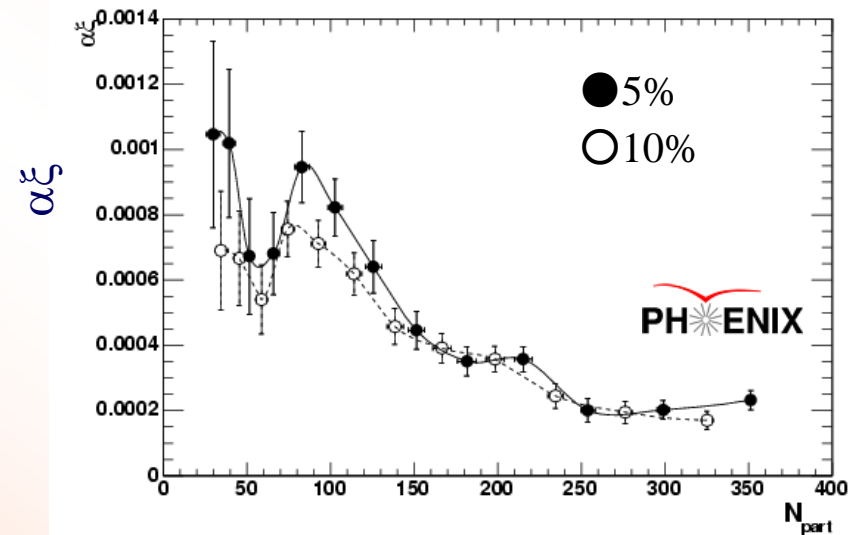
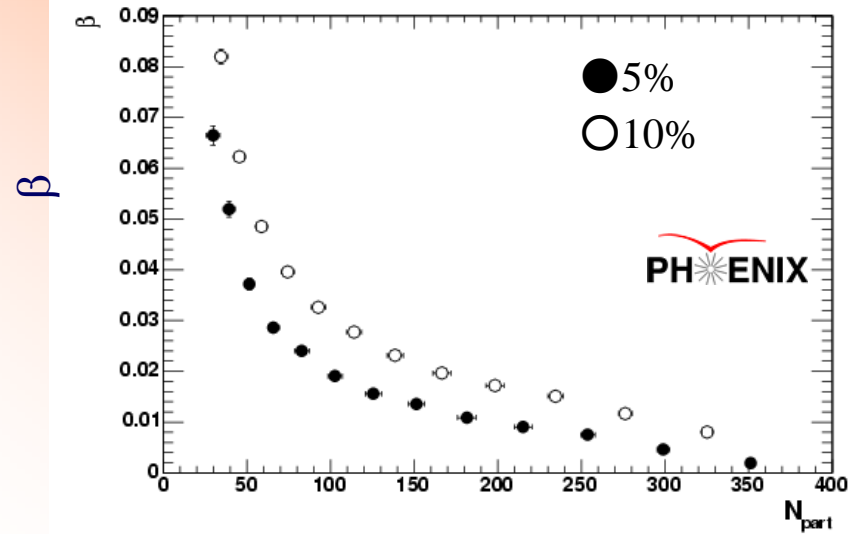
N_{part} dependence in Au+Au 200GeV

- β is systematically shift to lower values as the centrality bin width becomes smaller from 10% to 5%.
- This is understood as fluctuations of N_{part} for given bin widths.

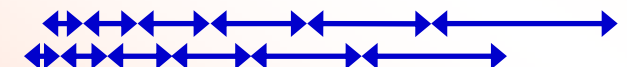
- $\alpha\xi$ product, which is monotonically related with the susceptibility $\chi_{k=0}$ of the system as,

$$\alpha\xi = \chi_{k=0} T / \bar{\rho}_1^2 \propto \bar{\rho}_1^{-2} \frac{T}{|T - T_C|}$$

- $\alpha\xi$ can be expected to decrease with increasing the number of participant or energy density.



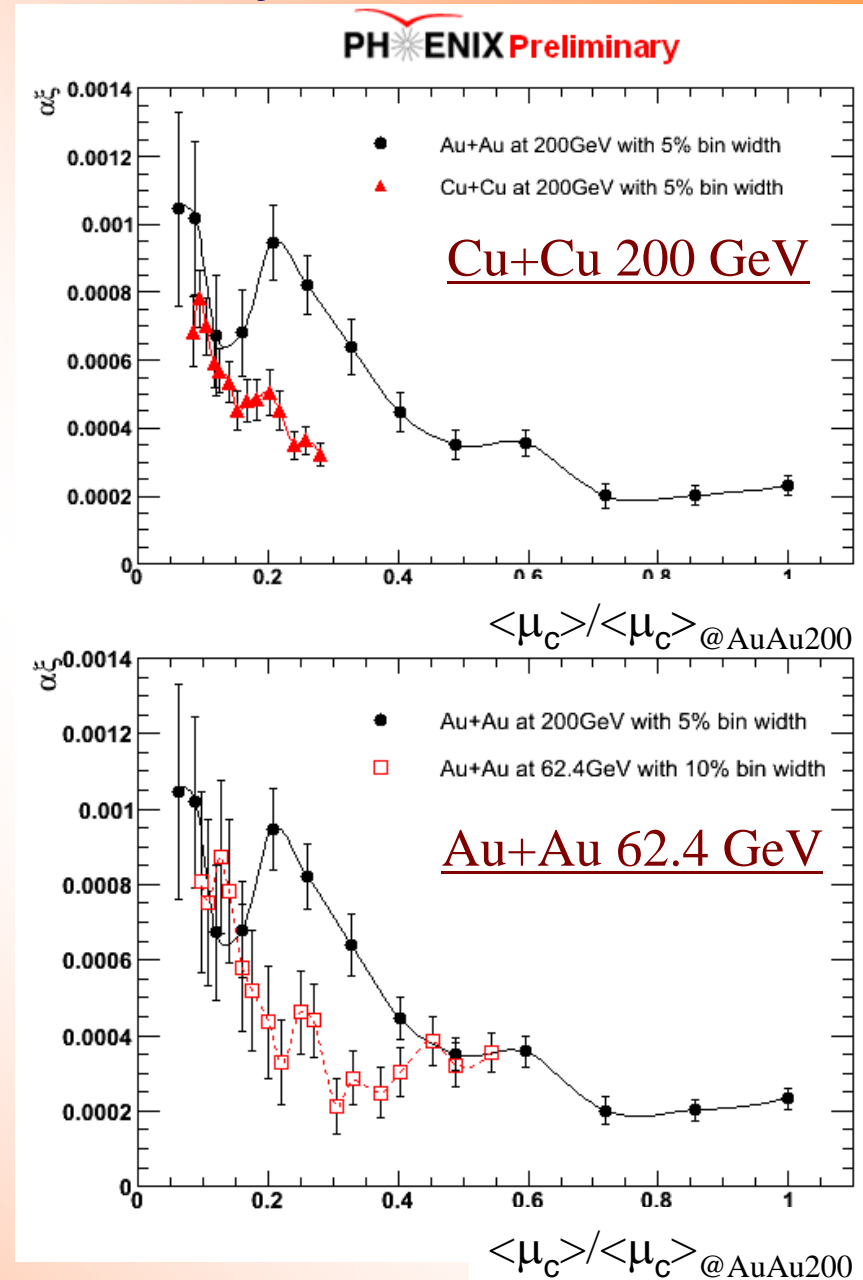
Centrality binning 5%



Centrality binning 10%

Comparison for three collision systems

- For the comparison horizontal axis is normalized mean multiplicity to that of top 5% in Au+Au 200GeV.
- The non-monotonic behavior in Au+Au 200 GeV, which is a possible critical behavior, is not seen at the Cu+Cu 200GeV and Au+Au 62.4 GeV.



Evaluations of $\alpha\xi$ non-monotonicity

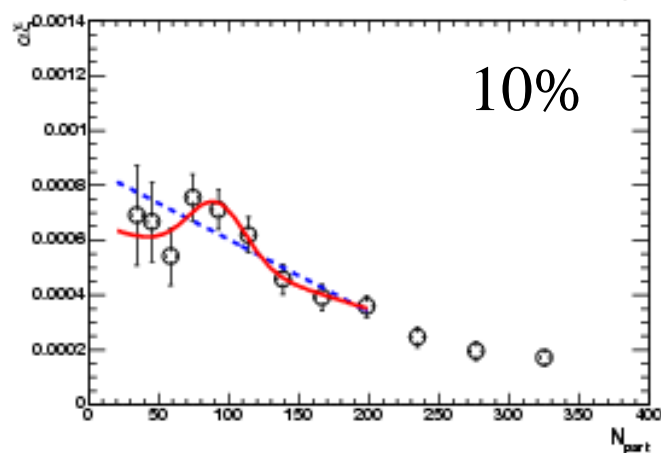
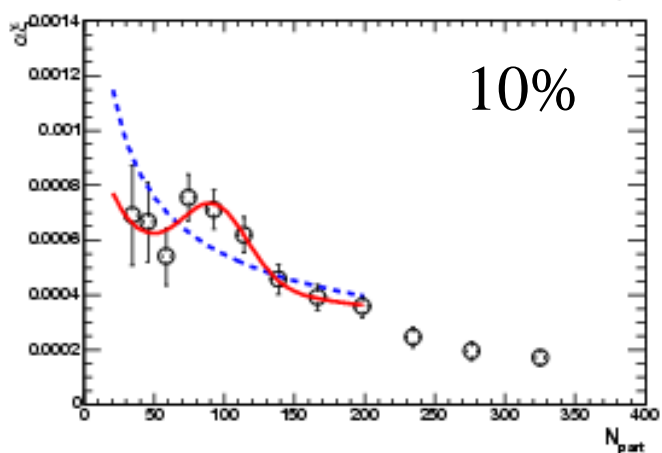
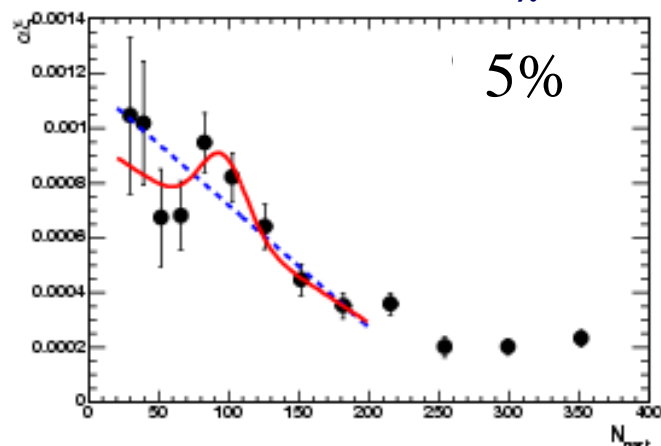
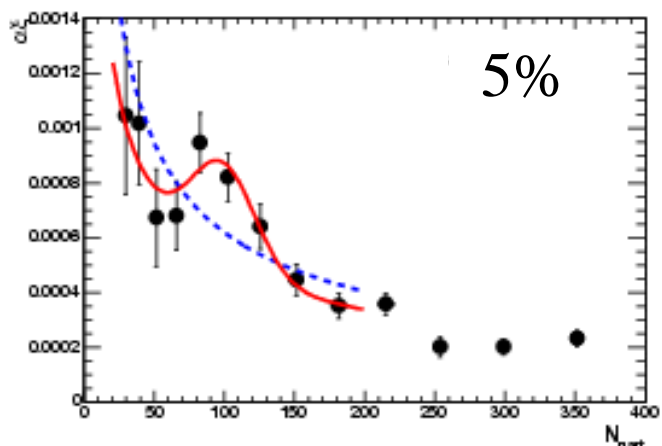
PHENIX: Phys. Rev. C76, 034903

$\chi^2/\text{NDF} = 2.76 : 0.60$

$\chi^2/\text{NDF} = 2.10 : 0.38$

Power law
Power law
+ Gaussian

Linear
Linear
+ Gaussian



$\chi^2/\text{NDF} = 1.23 : 0.79$

$\chi^2/\text{NDF} = 1.09 : 0.43$

Power law + Gaussian:

3.98 σ (5%), 3.21 σ (10%)

Linear + Gaussian:

1.24 σ (5%), 1.69 σ (10%)

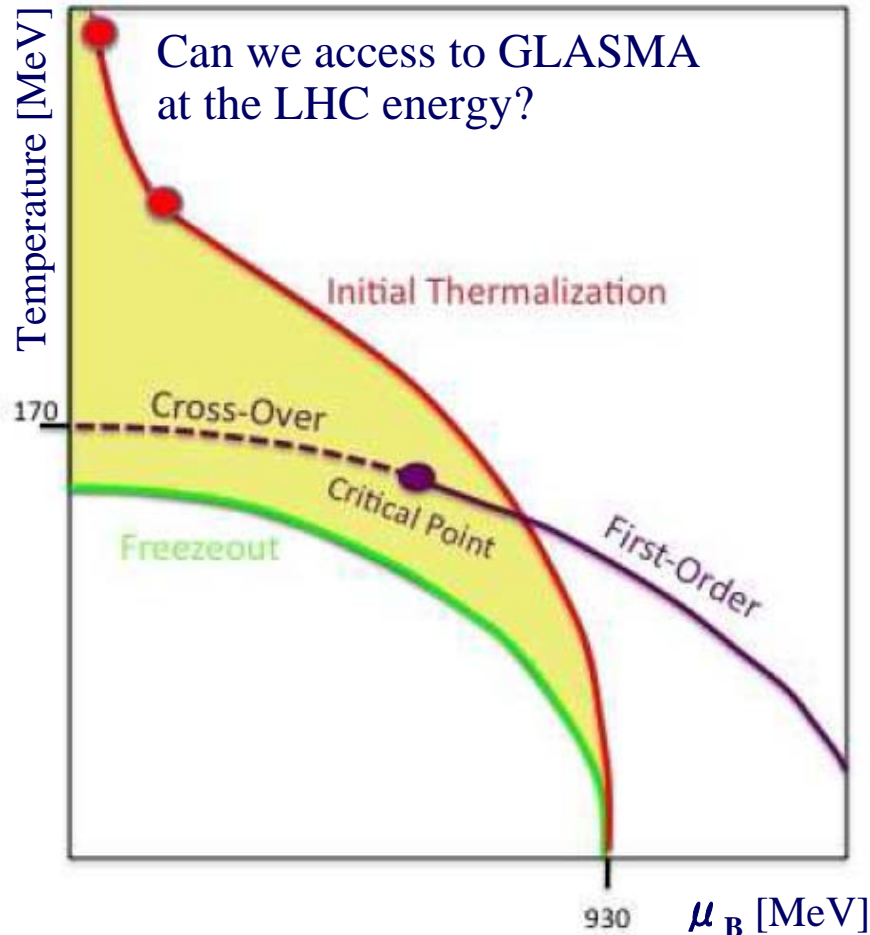
Summary

- **The multiplicity fluctuations** have been measured for all available datasets. It may be related the isothermal compressibility in grand canonical ensemble but no critical behavior was seen as a function of the centrality.
- **The longitudinal density correlations** have been measured via the functional form for pseudorapidity density fluctuations derived in the Ginzburg-Landau thermodynamical theory. The functional form can reasonably fit NBD k parameters as a function of pseudorapidity window sizes $\delta\eta$ not only for Au+Au 200 GeV but also for Cu+Cu 200 GeV and Au+Au 62.4 GeV.
- **The $\alpha\xi$ product** in the correlation function, which is monotonically related to susceptibility $\chi_{k=0}$ of the system, have been measured as a function of the number of participant nucleons N_{part} . No critical behavior was seen without any physical assumptions at the present precision.
- **A possible indication** of a local maximum is seen at $N_{part} \sim 90$ [$\epsilon_{Bj}\tau \sim 2.4 \text{ GeV}/(\text{fm}^{-2}\text{c})$] as compared to the power law baseline only for the Au+Au 200 GeV dataset. This might be a hint to search for the critical behavior at the QCD phase transition.
- **PHENIX** carries on to survey the multiplicity fluctuations for further different collision systems (5, 7, 39 GeV). Now we are taking the data at RHIC Run10.

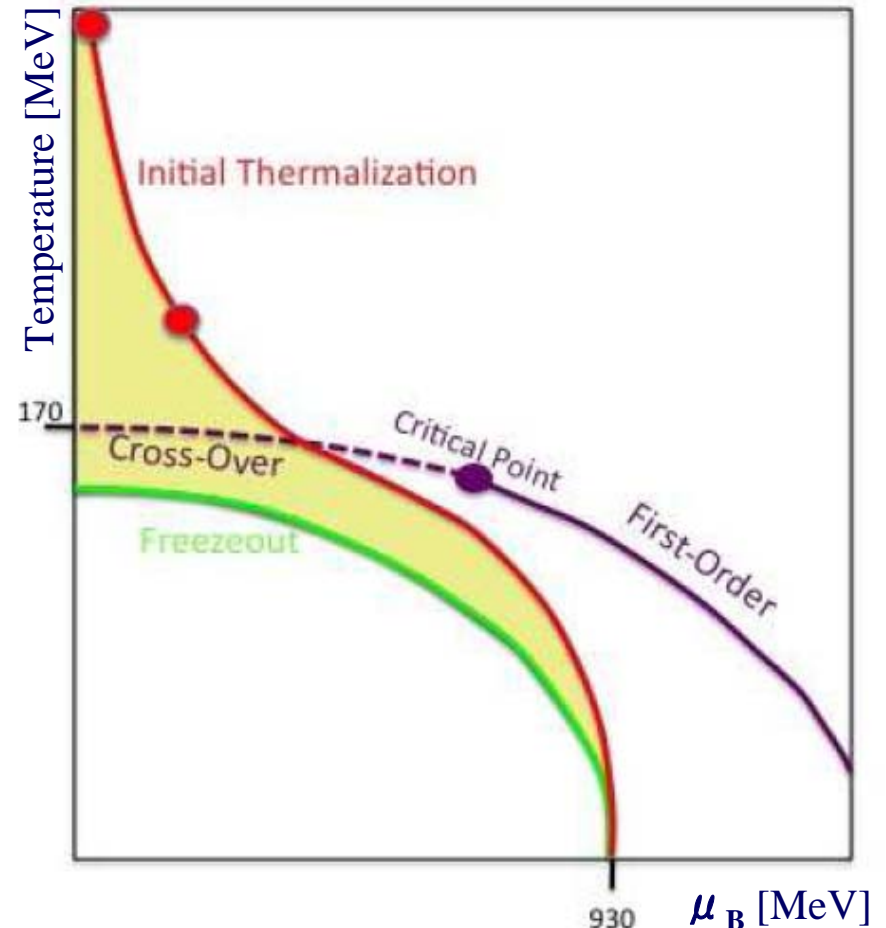
Backup

Mapping on QCD phase diagram

We can find the signature of CEP by the energy scan at RHIC.

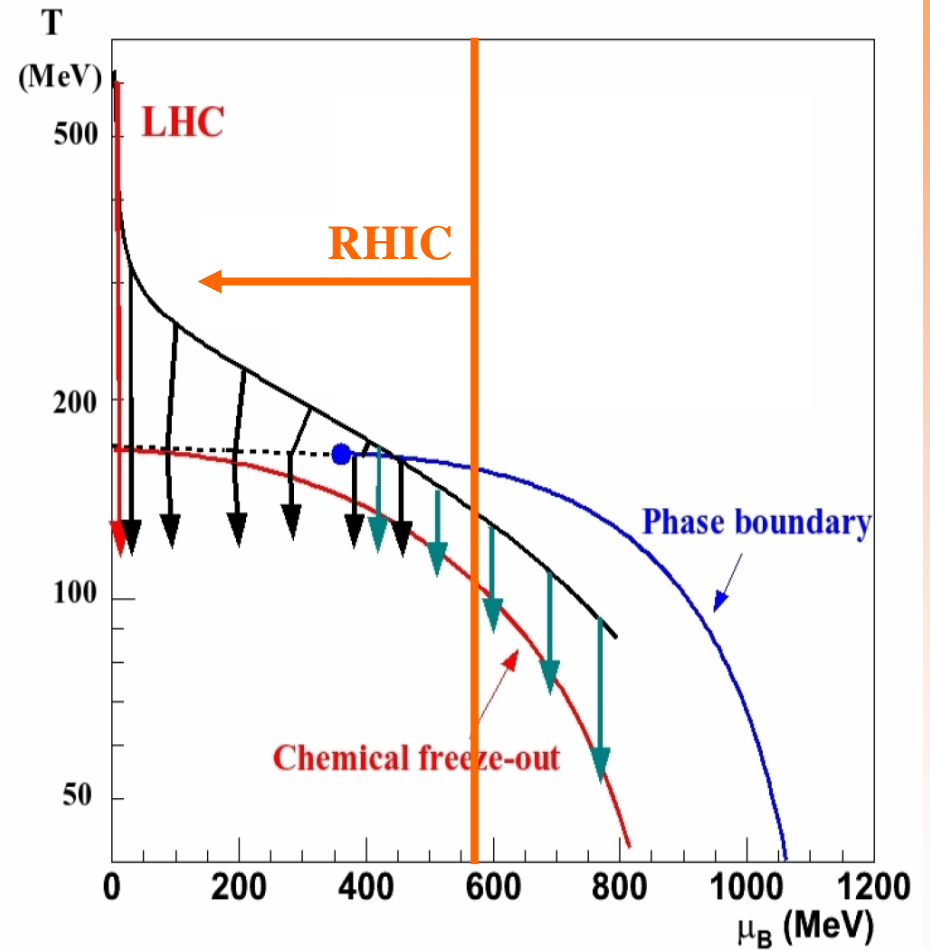
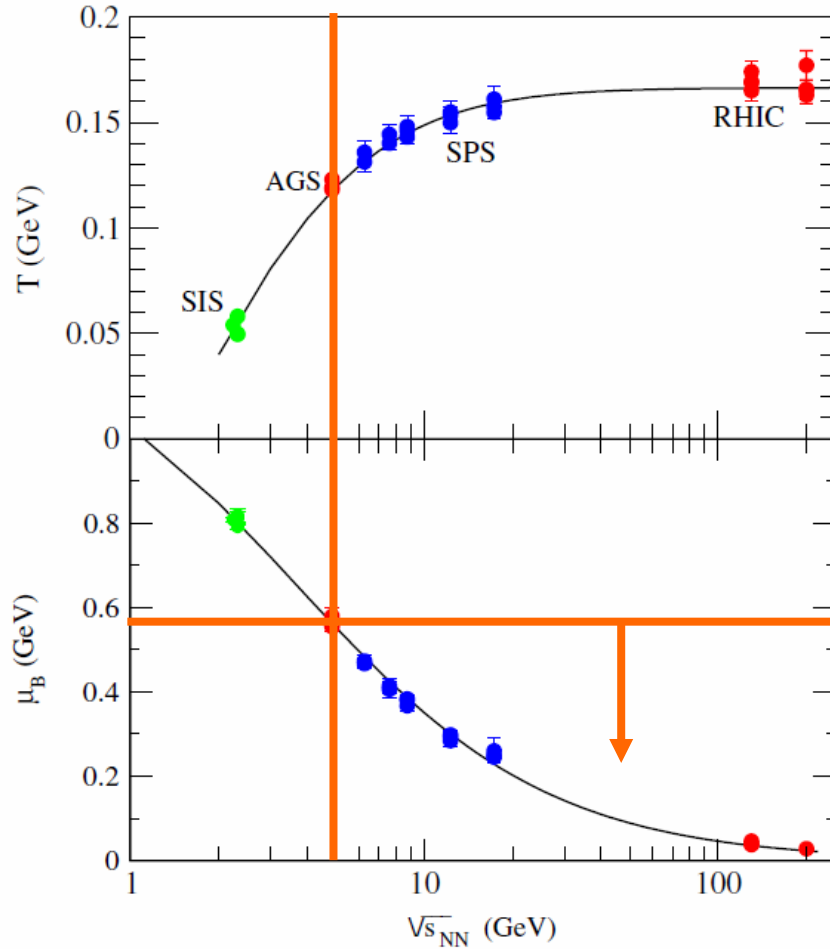


Bad case, we can not access to the CEP by the accelerator.



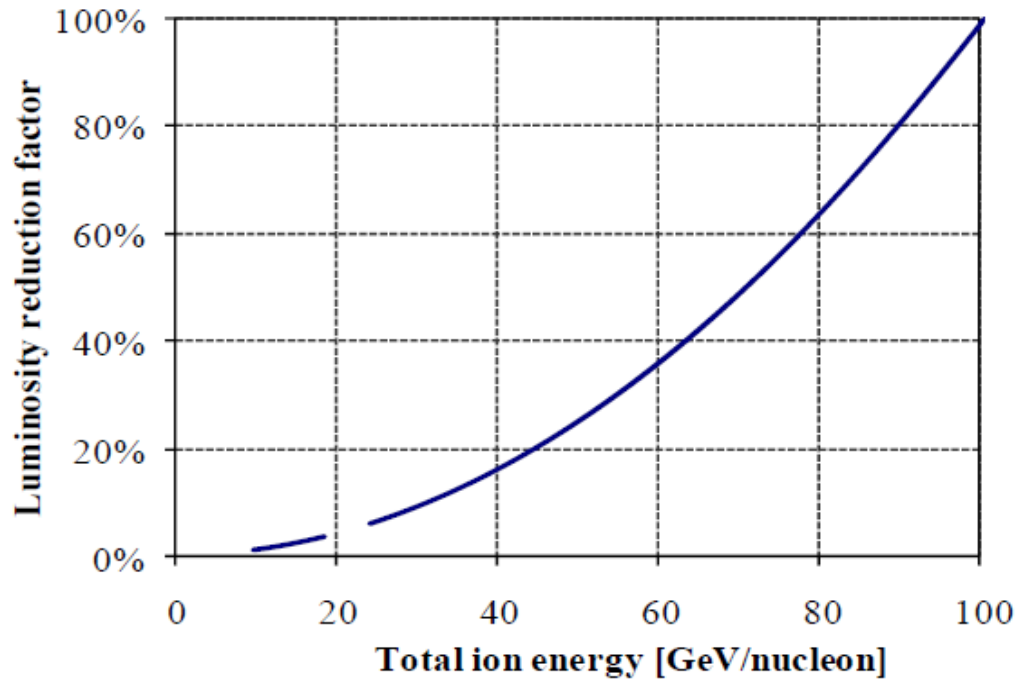
Energy scan at RHIC

Chemical freeze-out temperature



J. Cleymann et al. Phys. Rev. C73, 034905.

Low energy capability at RHIC



W. Fischer et. al. (RHIC)

$\sqrt{s_{NN}}$ [GeV]	μ_B [MeV]	$\langle \text{Event Rate} \rangle$ [Hz]	Days/ million events	No of events	No of beam days (setup+physics)
5.0	535	0.7	21	5M	5+105
6.1	470	1.4	11.3	5M	4+57
7.7	405	2.7	5.7	5M	3+29
8.8	370	4	3.9	5M	2+19
12	295	—	—	—	—
18	210	>30	0.5	5M	1+3
28	145	>60	<<1	5M	2+1

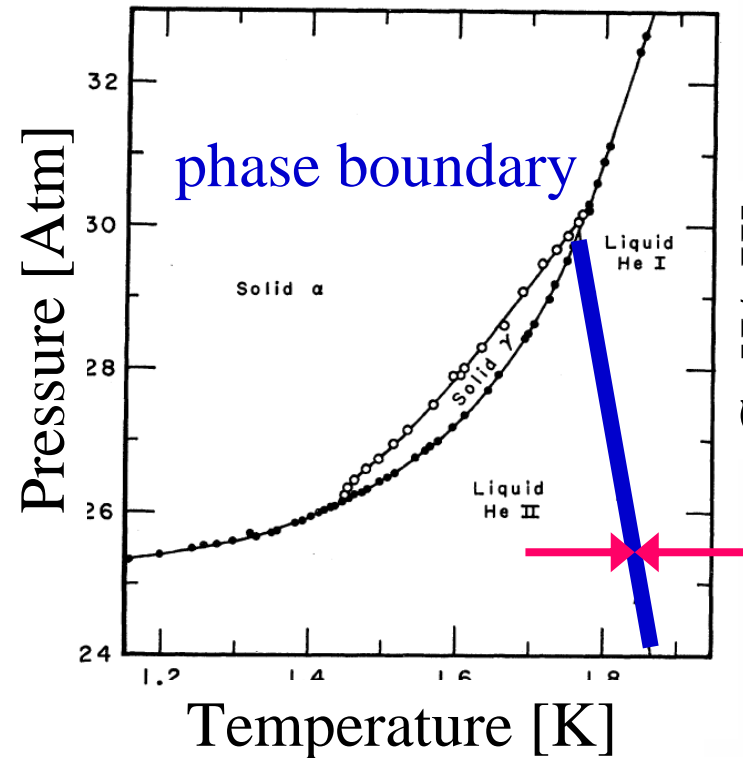
- RHIC can operate by 5GeV through 200GeV (collision energy) with the heavy-ion mode.

- Since almost of the fluctuation observables are focusing on the low p_T particles, several million events are enough statistics for the measurements and analysis.

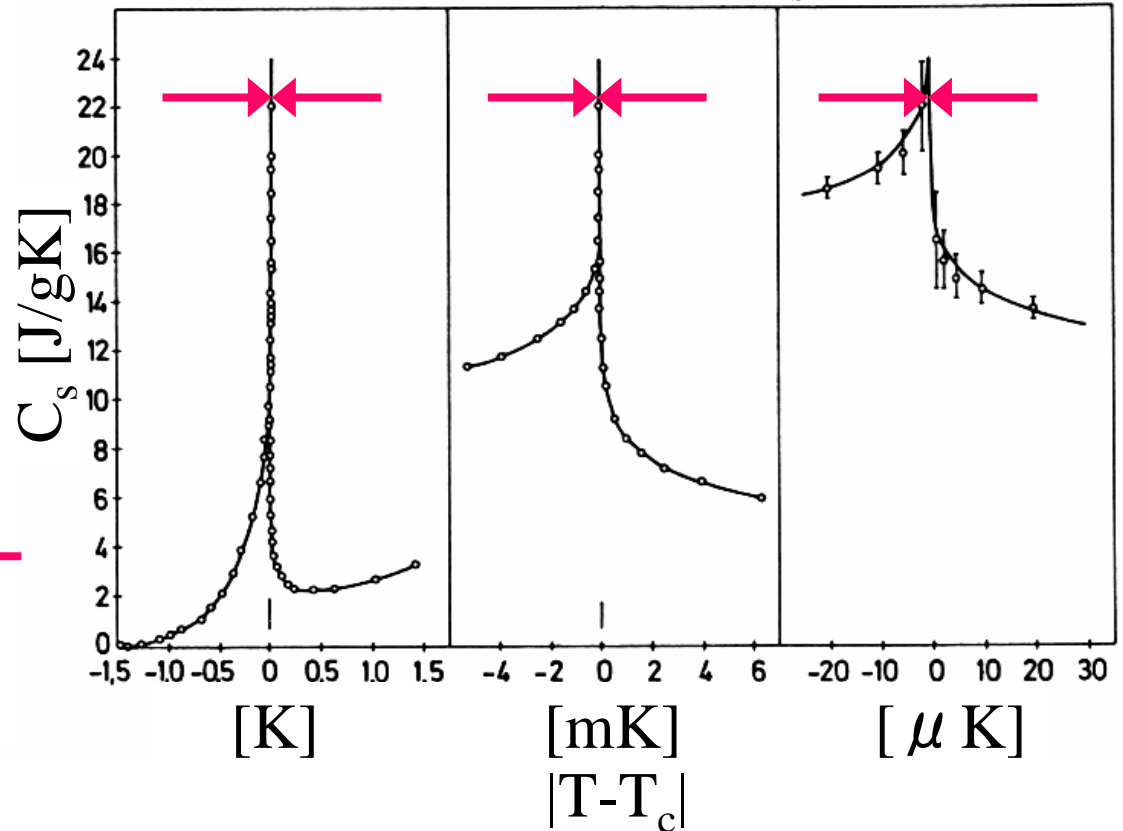
- That can be corrected by several weeks.

Analogy of the phase transition in He⁴

He⁴ phase diagram



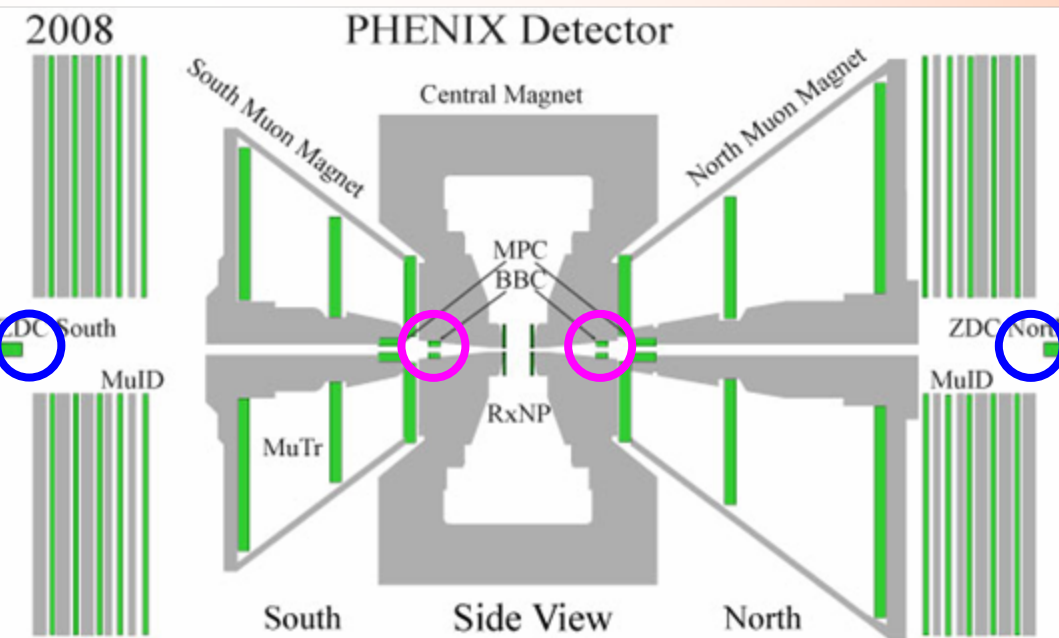
Specific heat C_s



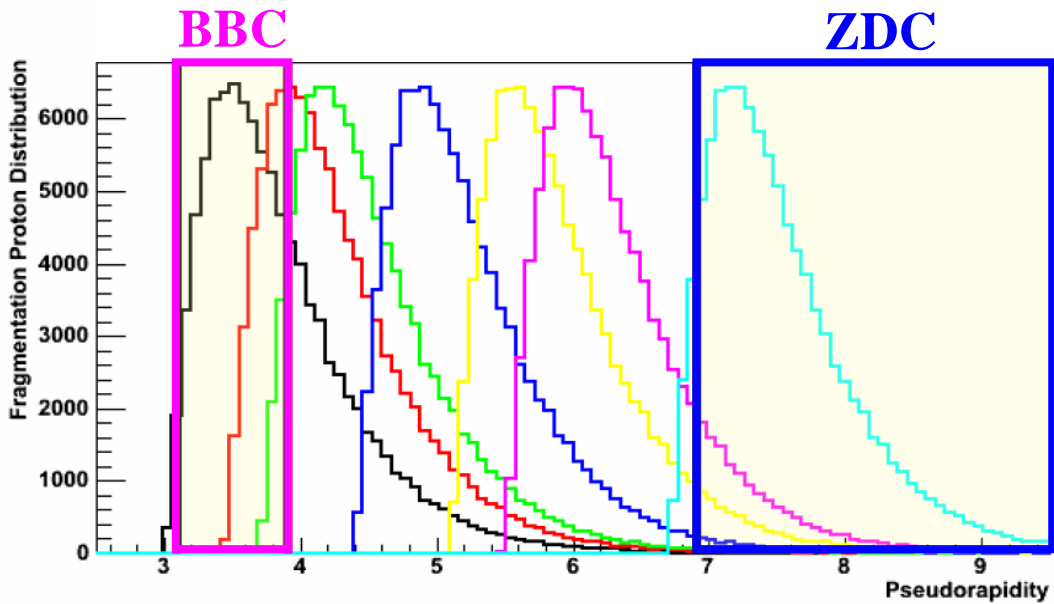
W. M. Fairbank and M. J. Buckingham, Int. Conf. on Low Temp. Phys. (1957)

$$\chi = -\left(\frac{\partial \Phi}{\partial h}\right) = -\left(\frac{\partial^2 F}{\partial h^2}\right)$$

Triggers for low energy collision at PHENIX



- Fermi motion may allow a significant fraction of spectator protons or light nuclei to hit the PHENIX BBC. PHENIX is continuing to study the model dependencies of such findings and whether the BBC counter is sufficient for triggering.



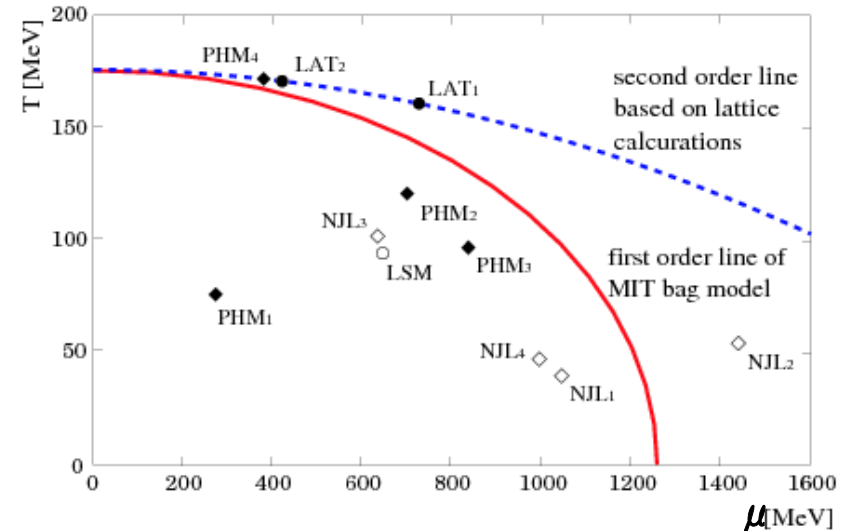
H. Pereira and J. Nagle
(URQMD based analysis)

5, 7.7, 10, 20, 40, 60, 200 GeV

Physics Motivation

The second order phase transition is predicted at $\mu=0$ and $T>0$ by the lattice QCD calculation at zero mass, $m=0$. Since actual quarks have been thought having a finite current mass, a smooth crossover transition is expected due to the finite masses of quarks at $\mu=0$ and $T>0$ and $m\neq 0$. The crossover transition is also predicted by the lattice QCD calculation. Thus, logically one can expect that a critical end-point (CEP) exists at the end of the first order phase transition line.

According to this picture, the CEP is defined by the connecting point of the two second order lines and one first order line in the $m=0$ plane. Consequently, the location of the CEP would be the landmark in understanding the whole structure of the phase diagram. Figure shows the predictions of the CEP locations based on the lattice QCD calculations, the NJL models, the linear sigma model and the other phenomenological models. Dashed line is the expected second order phase boundary obtained by connecting two CEPs in the different lattice QCD calculations and the transition temperature at $\mu=0$. Although numerical calculations using the lattice gauge theory as well as model calculations predict the existence of the CEP, none of them have reached a quantitative agreement on the location at the present precision.

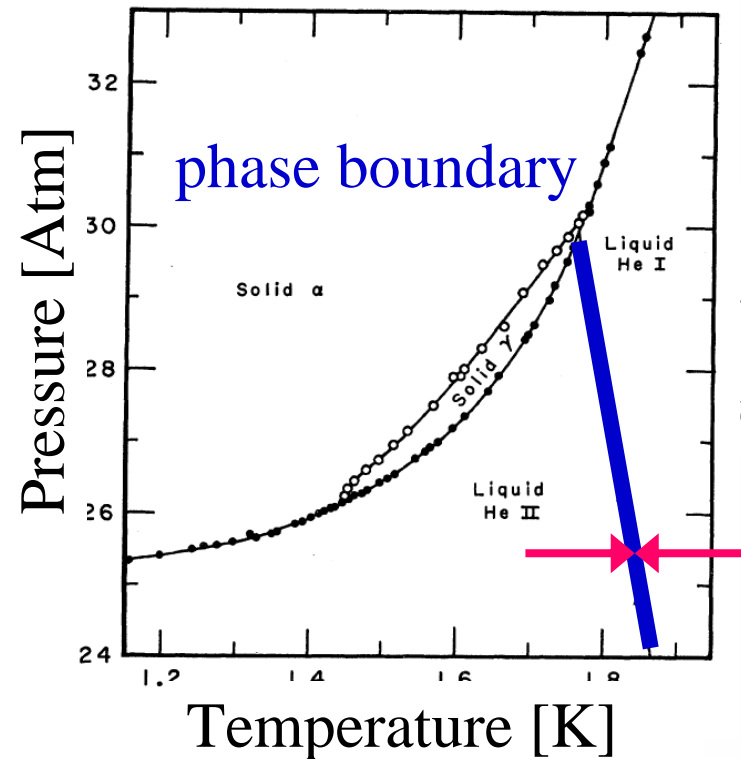


[M. A. Stephanov, *Int. J. Mod. Phys. A*20, 4387 (2005)]

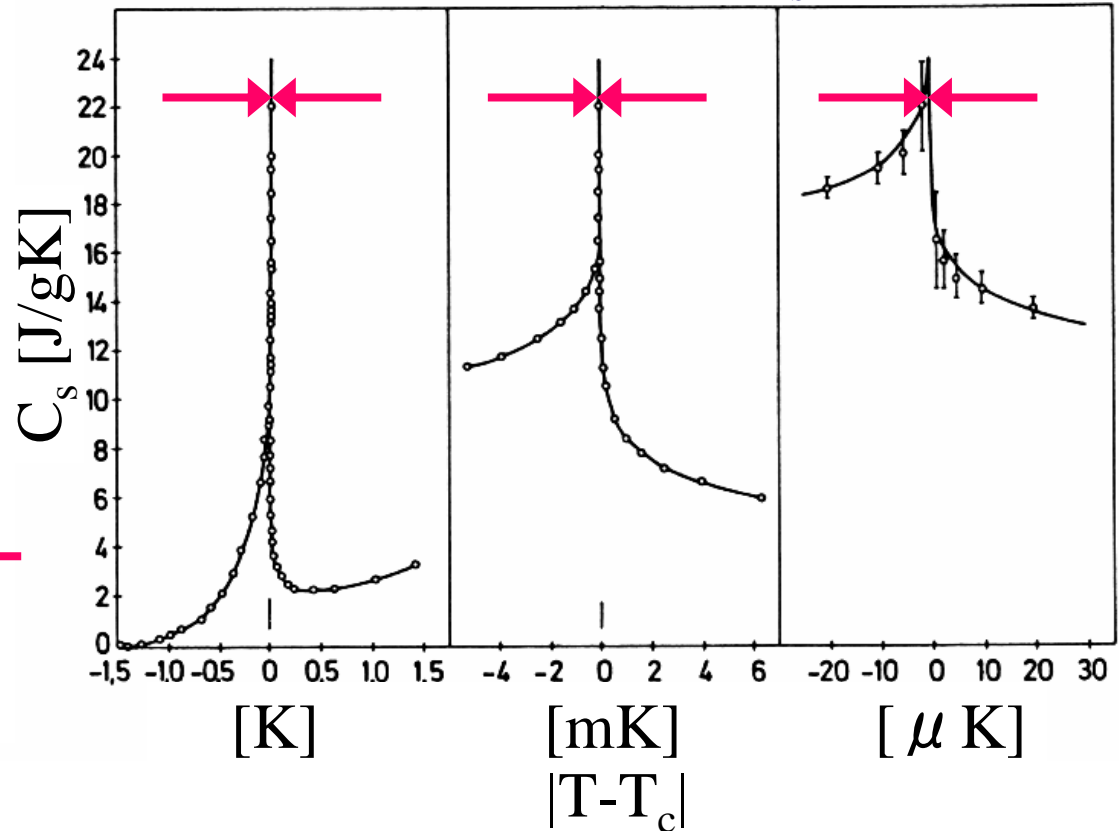
Therefore, experimental investigations are indispensable to pin down the location of the CEP and phase boundary to investigate properties of the phase structure in the QCD energy scale based on fundamental observables.

Analogy of the phase transition in He⁴

He⁴ phase diagram



Specific heat C_s



[W. M. Fairbank and M. J. Buckingham, Int. Conf. on Low Temp. Phys. (1957)]

Here is one of the most obvious examples of phase transitions. Figure shows the phase diagram of He⁴ as a function of pressure and temperature. The phase indicated by "Liquid He II" is the known super fluidity phase. The specific heat, which corresponds to the second order derivative indicates the divergence at $T=T_c$. Therefore, the line with triangles corresponds to the second order phase transition line.

Possible observables (signature of phase transition)

Second-order derivative free energy

$$\chi = -\left(\frac{\partial\Phi}{\partial h}\right) = -\left(\frac{\partial^2 F}{\partial h^2}\right)$$

Susceptibility: e.g. specific heat, compressibility, correlation length

Ginzburg-Landau phenomenology

• Order parameter: density fluctuation $\phi(r) = \rho(r) - \langle\rho\rangle$

• Two point correlation function $G_2(r_1, r_2) \equiv \langle(\rho(r_1) - \langle\rho\rangle)(\rho(r_2) - \langle\rho\rangle)\rangle$

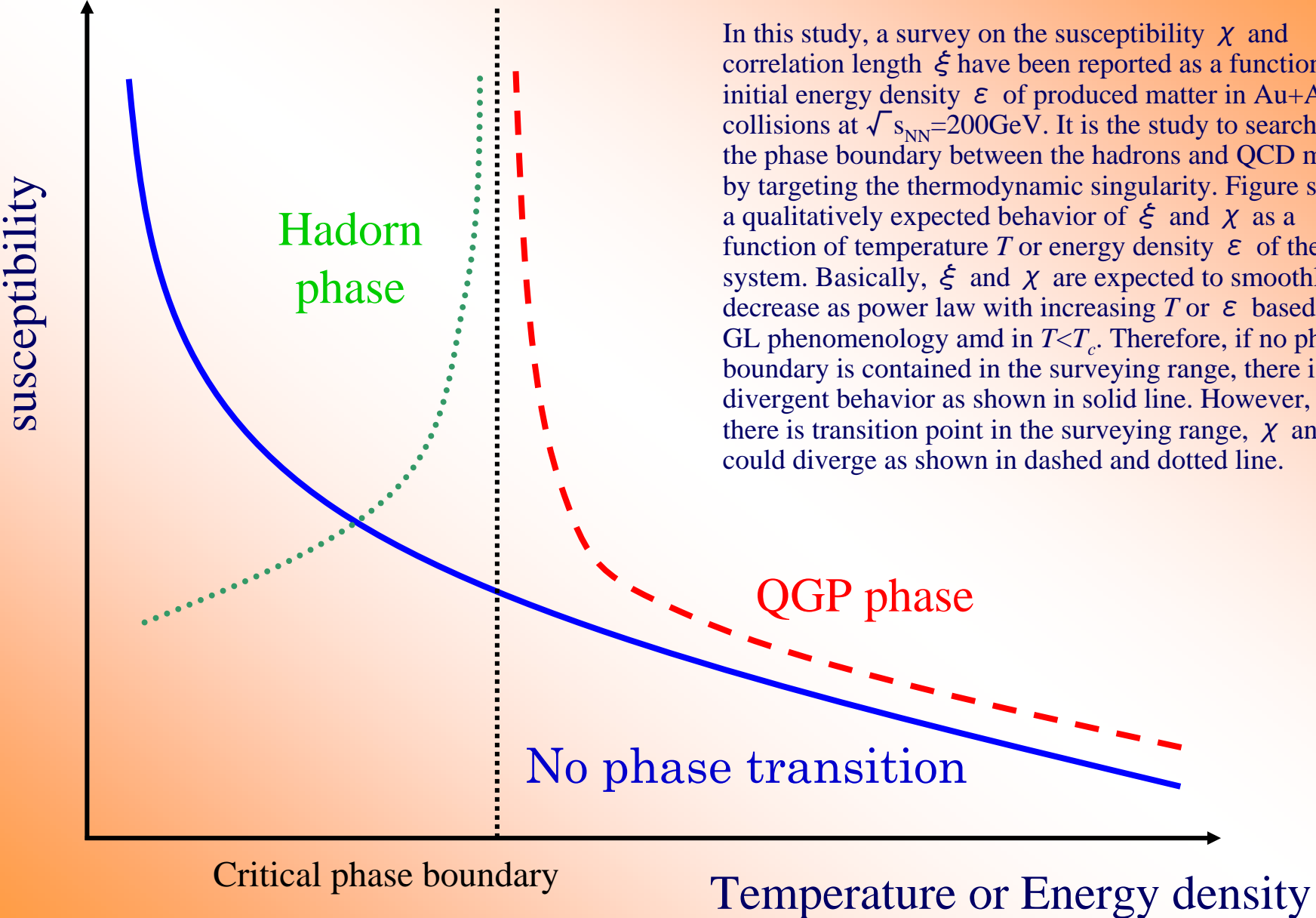
• Correlation length

$$G_2 \propto e^{-|r|/\xi(T)}, \quad \xi(T) \propto \frac{1}{|T - T_c|}$$

• Susceptibility

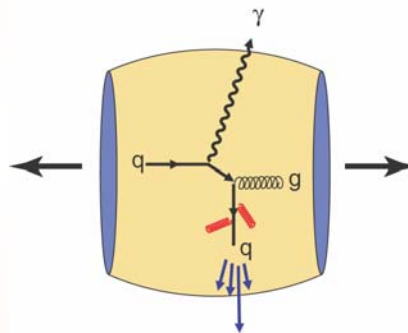
$$\chi_k \propto \frac{1}{|T - T_c| (1 + k^2 \xi(T)^2)}$$

Case with the high energy heavy ion collisions



In this study, a survey on the susceptibility χ and correlation length ξ have been reported as a function of initial energy density ϵ of produced matter in Au+Au collisions at $\sqrt{s_{NN}}=200\text{GeV}$. It is the study to search for the phase boundary between the hadrons and QCD matter by targeting the thermodynamic singularity. Figure shows a qualitatively expected behavior of ξ and χ as a function of temperature T or energy density ϵ of the system. Basically, ξ and χ are expected to smoothly decrease as power law with increasing T or ϵ based on GL phenomenology and in $T < T_c$. Therefore, if no phase boundary is contained in the surveying range, there is no divergent behavior as shown in solid line. However, if there is transition point in the surveying range, χ and ξ could diverge as shown in dashed and dotted line.

Is medium dense enough?



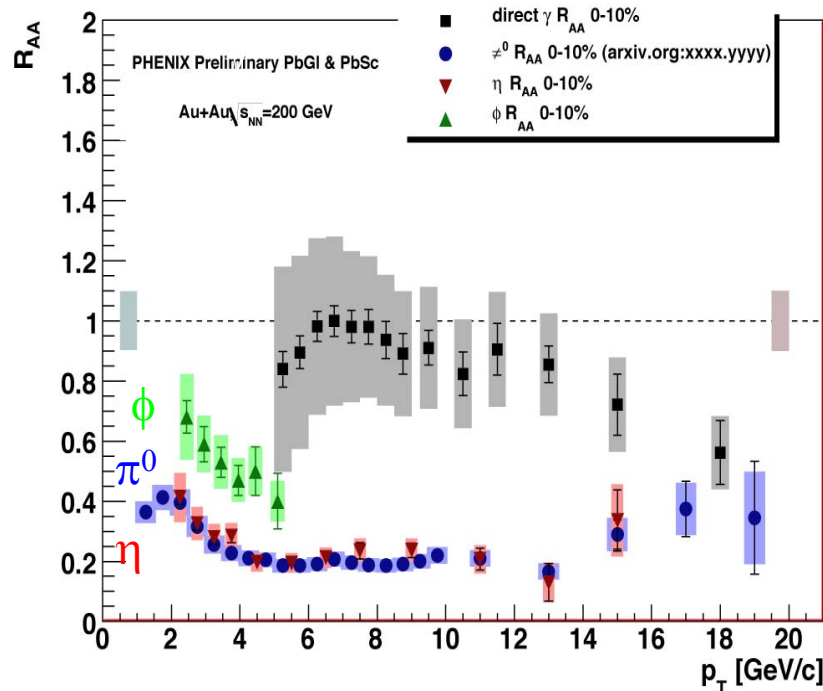
Nuclear Modification Factor

$$R_{AA} \equiv \frac{d^2 N^{AA} / dy dp_T}{d^2 N^{pp} / dy dp_T \cdot \langle N_{coll}^{AA} \rangle}$$

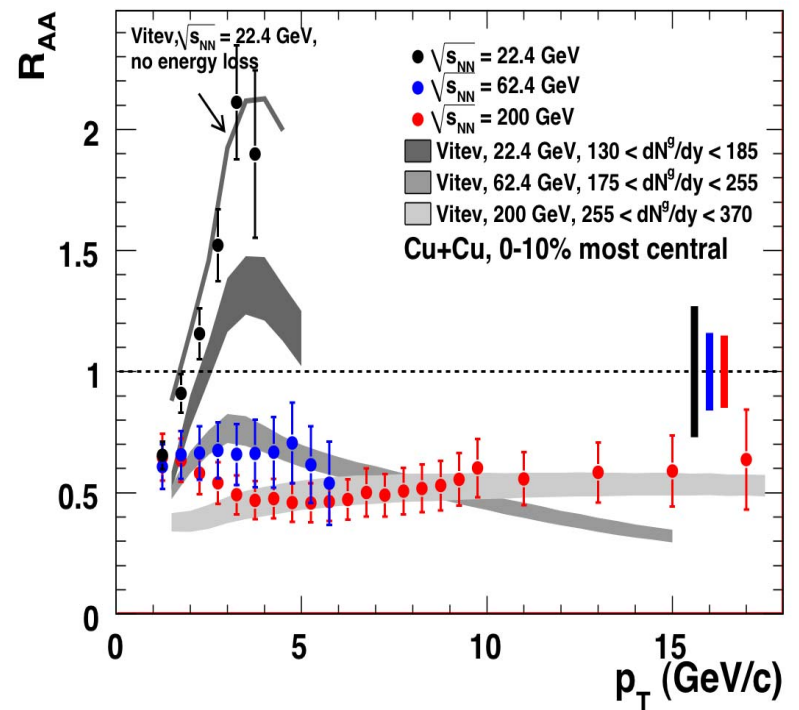
Particle Species

Energy

π^0 Au+Au 200 GeV (Run 4)

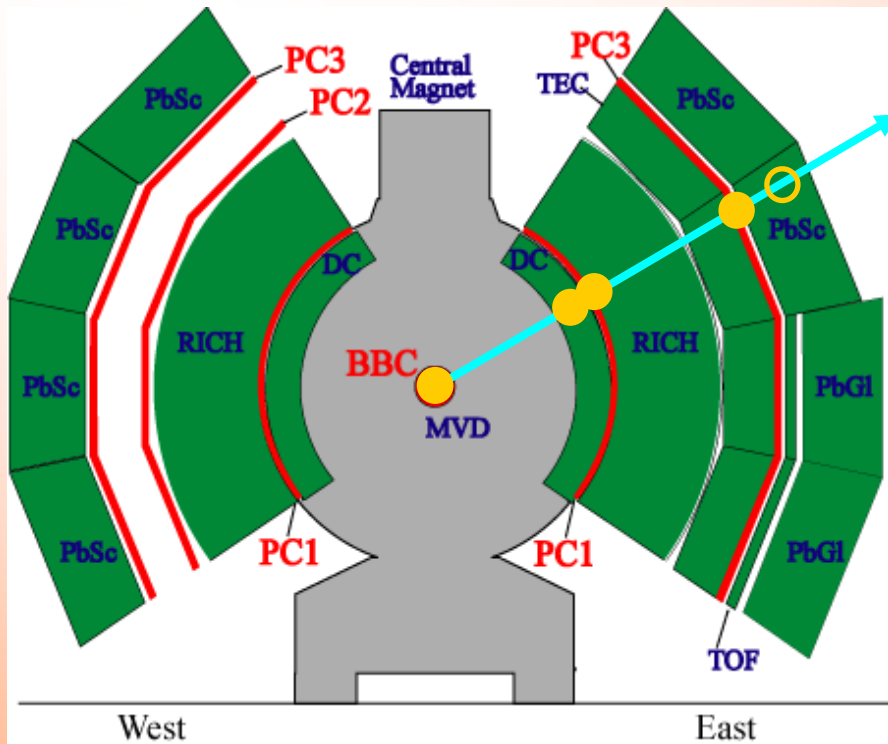


π^0 Cu+Cu 22,62,200 GeV (Run 5)



arXiv:0801.4555

Measurement of charged particles at PHENIX



- Acceptance: $\Delta \eta < 0.7$, $\Delta \phi < \pi/2$
- Track identification: DC
- Track association: beam vertex (BBC), hit point in wire chamber (PC1, PC3), Cluster position in EMC.

- Measuring tracks at no magnetic field condition to optimize low momentum charged particles.

- Minimum p_T threshold.

- π : 0.1 GeV/c
- K : 0.25 GeV/c
- p : 0.35 GeV/c

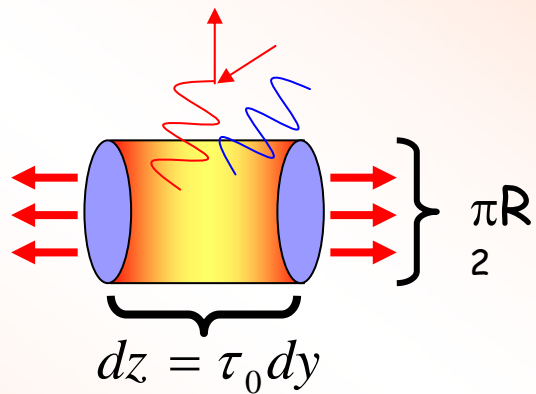
- Particle composition.

- π : K : p = 94 : 4 : 2

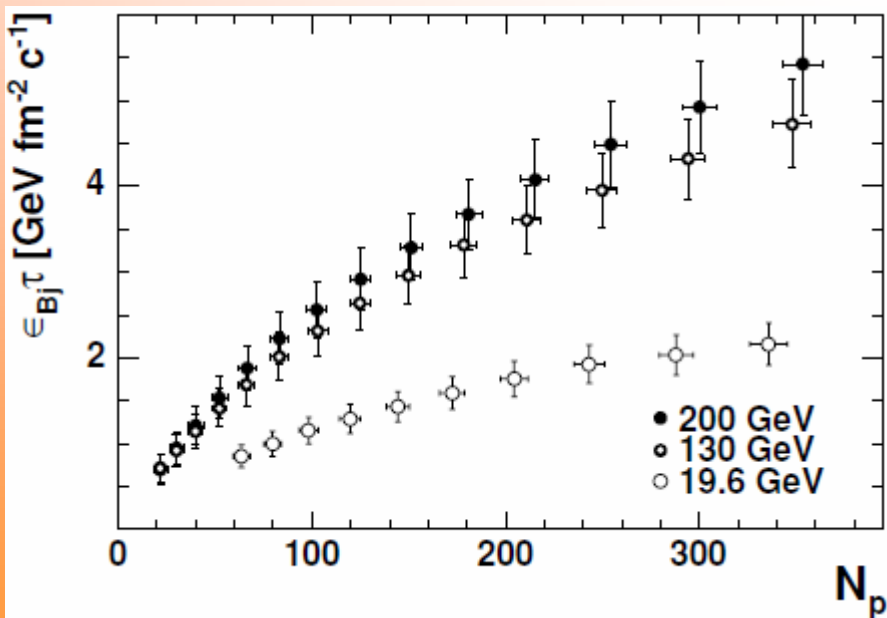
- Mean p_T for $\pi = 0.57$ GeV/c.

- For inclusive charged particle, maximum 3 % difference at $\eta = 0.35$ for the conversion of rapidity to pseudo rapidity.

Is initial temperature high enough?

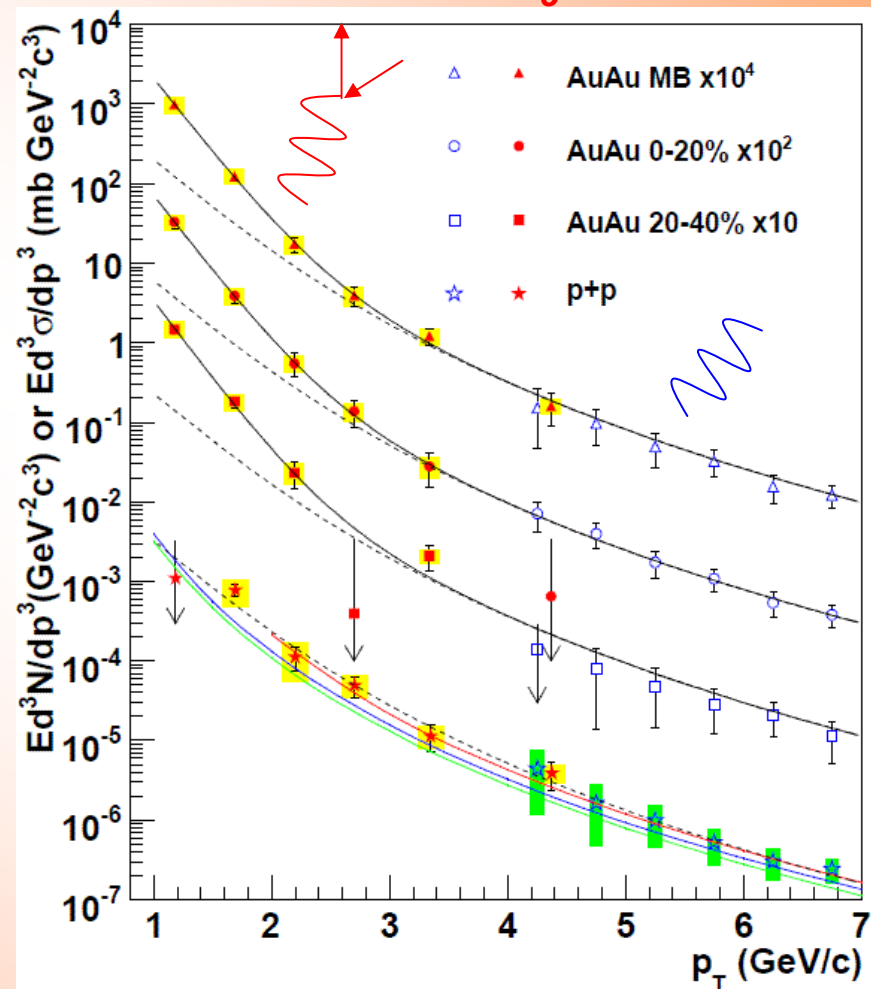


$$\varepsilon_{Bj} = \frac{1}{\pi R^2} \frac{1}{\tau_0} \frac{dE_T}{dy}$$



PHYSICAL REVIEW C 71, 034908 (2005)

In central Au+Au collision
 $T = 221 \pm 23(\text{stat}) \pm 18(\text{sys})$
 Lattice result $T_c \sim 170 \text{ MeV}$



arXiv:0804.4168v1 [nucl-ex] 25 Apr 2008

Density-density correlation in longitudinal space

Longitudinal space coordinate z can be transformed into rapidity coordinate in each proper frame of sub element characterized by a formation time τ at which dominant density fluctuations are embedded.

$$z = \tau \sinh(y)$$

$$t = \tau \cosh(y)$$

$$dz = \tau \cosh(y) dy$$

Due to relatively rapid expansion in y , analysis in y would have an advantage to extract initial fluctuations compared to analysis in transverse plane in high energy collision.

$$g(T, \phi, h) - g_0 = \int_{\delta y} dy \int_{s_{\perp}} d^2 x_{\perp} \left[\frac{1}{2\tau^2 \cosh(y)} \left(\frac{\partial \phi}{\partial y} \right)^2 + \cosh(y) \left(\frac{1}{2} (\nabla_{\perp} \phi)^2 + U(\phi) \right) \right]$$

In narrow midrapidity region like PHENIX, $\cosh(y) \sim 1$ and $y \sim \eta$.

Direct observable for Tc determination

GL free energy density g with $\phi \sim 0$ from high temperature side is insensitive to transition order, but it can be sensitive to Tc

$$g(T, \phi, h) = g_0 - \frac{1}{2} A(T) (\nabla \phi)^2 + \frac{1}{2} a(T) \phi^2 + \frac{1}{4} b \phi^4 + \frac{1}{6} c \phi^6 \dots - h \phi$$

spatial correlation ϕ disappears at Tc $\rightarrow a(T) = a_0(T - T_c)$

Fourier analysis on

$$G_2(y) = \langle \phi(0) \phi(y) \rangle$$

$$\langle |\phi_k|^2 \rangle = Y \int G_2(y) e^{-ik(y)} dy$$

$$\langle |\phi_k|^2 \rangle = \frac{NT}{Y} \frac{1}{a(T) + A(T)k^2}$$

Susceptibility

$$\chi_k = \frac{\partial \phi_k}{\partial h} \propto \left(\frac{\partial^2 (g - g_0)}{\partial \phi_k^2} \right)^{-1} = \frac{1}{a_0(T - T_c)(1 + k^2 \xi^2)}$$

Susceptibility in long wavelength limit

$$\chi_{k=0} = \frac{1}{a_0(T - T_c)} \propto \frac{\xi}{T} G_2(0)$$

1-D two point correlation function

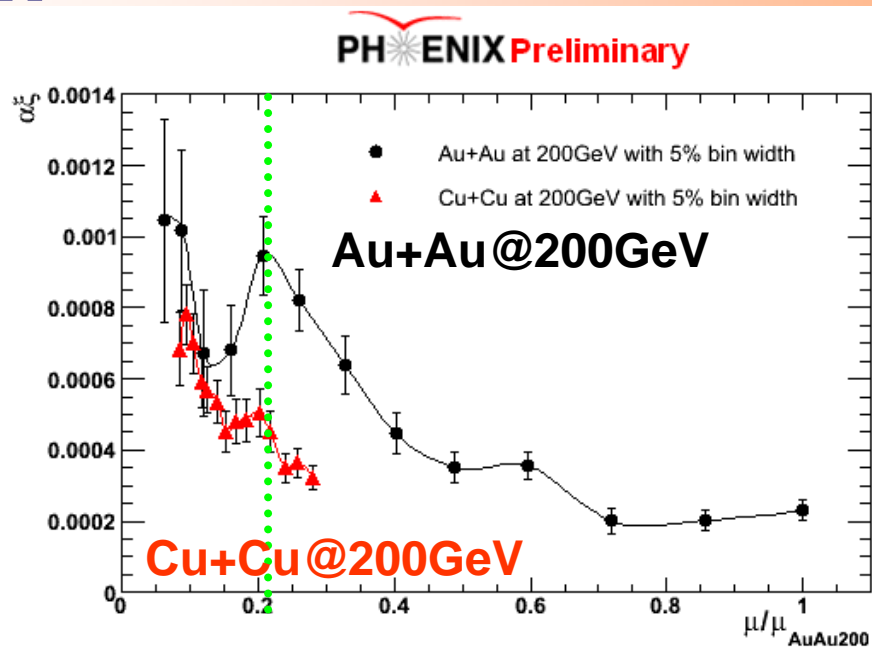
$$G_2(y) = \frac{NT}{2Y^2 A(T)} \xi(T) e^{-|y|/\xi(T)}$$

Correlation length

$$\xi(T)^2 \equiv \frac{A(T)}{a_0(T - T_c)}$$

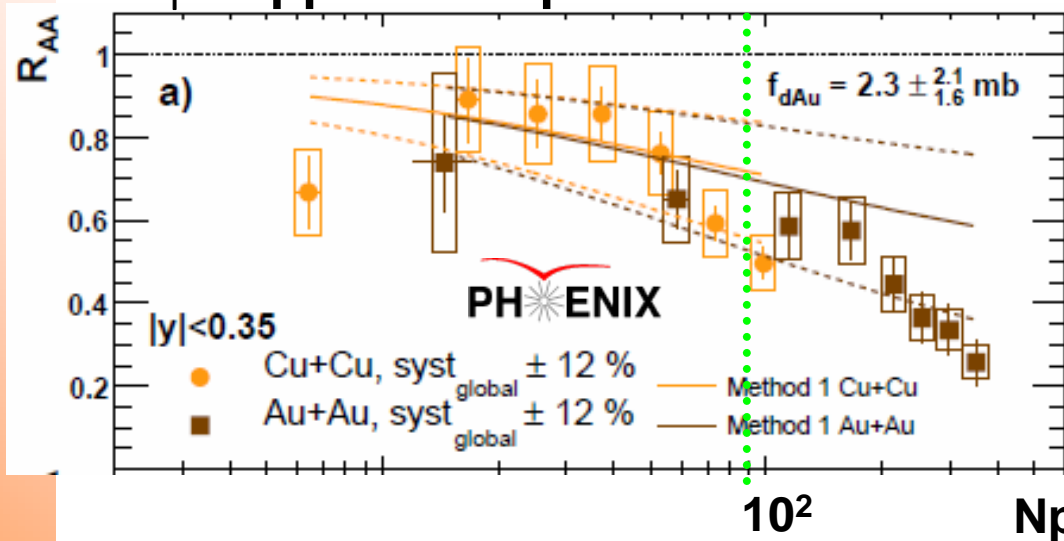
Product between correlation length and amplitude can also be a good indicator for $T \sim T_c$

How about $\langle cc \rangle$ suppression?



$N_{\text{part}} \sim 90$ in
AuAu@200GeV
 $\epsilon_{\text{BJT}} \sim 2.4 \text{ GeV}/\text{fm}^2/c$

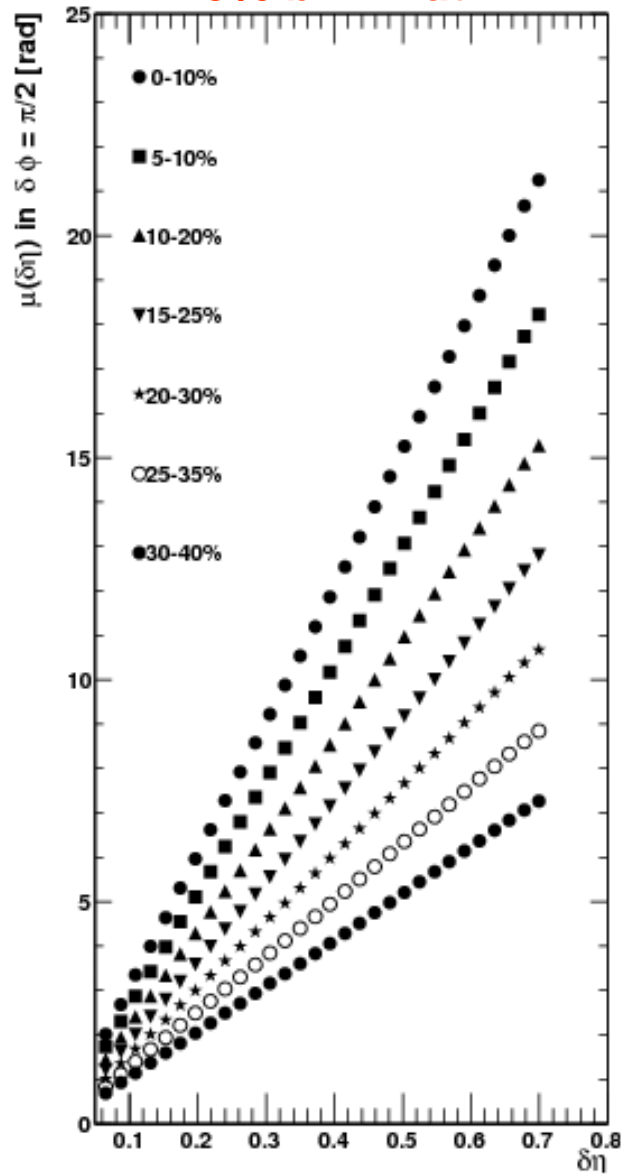
J/ψ suppression pattern



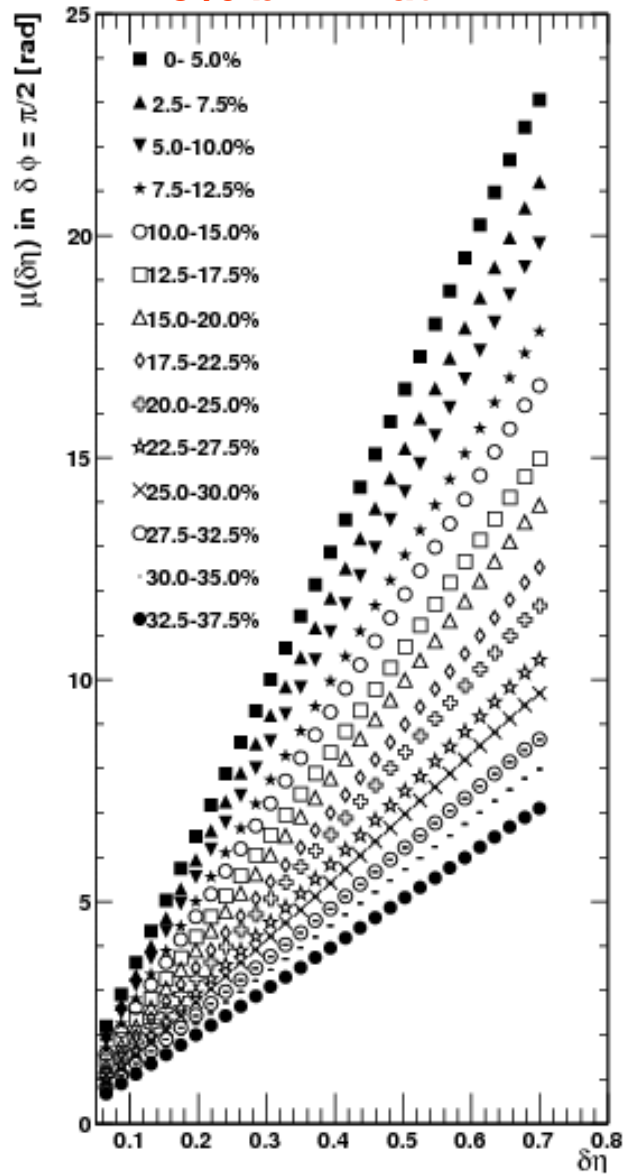
[arXiv:0801.0220v1 \[nucl-ex\]](https://arxiv.org/abs/0801.0220v1)

Corrected mean multiplicity $\langle \mu_c \rangle$

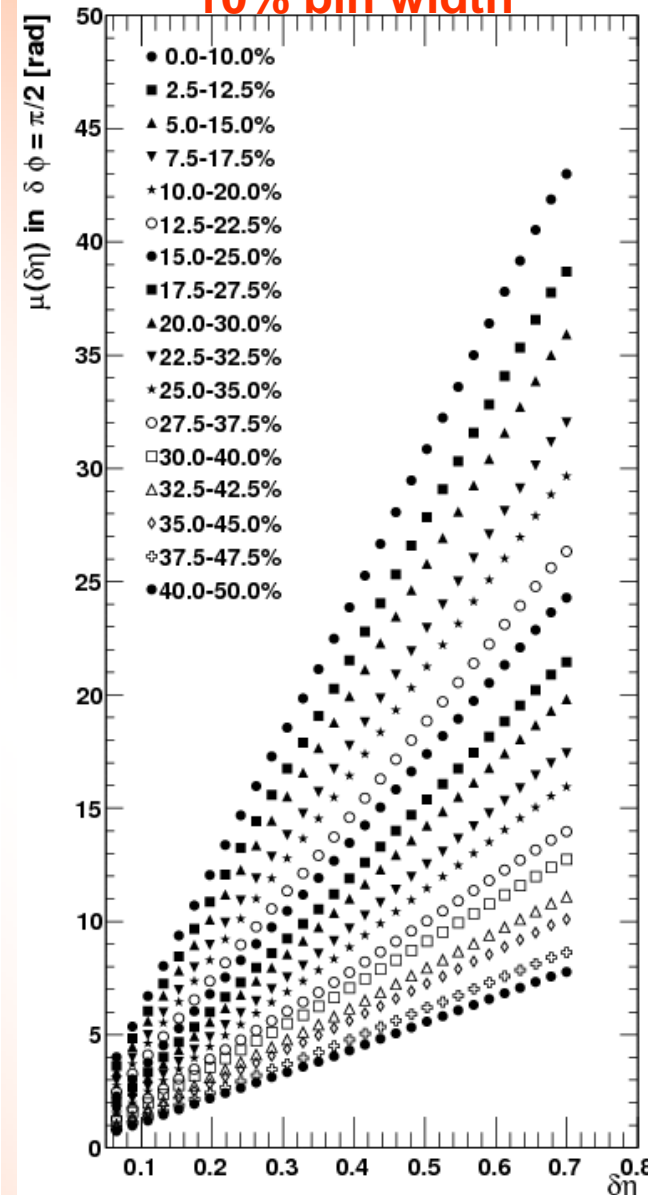
Cu+Cu@200GeV
10% bin width



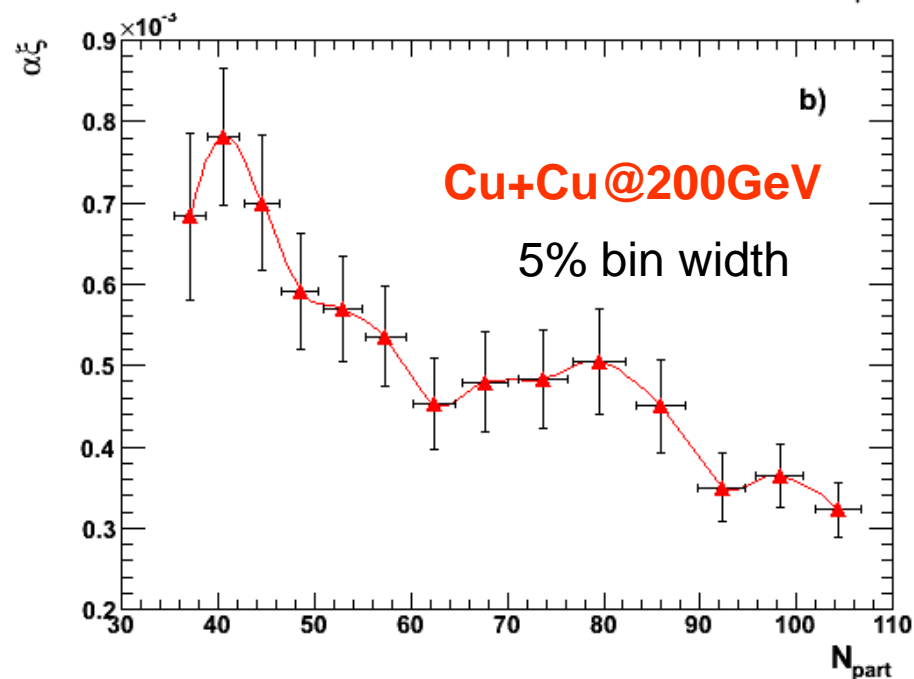
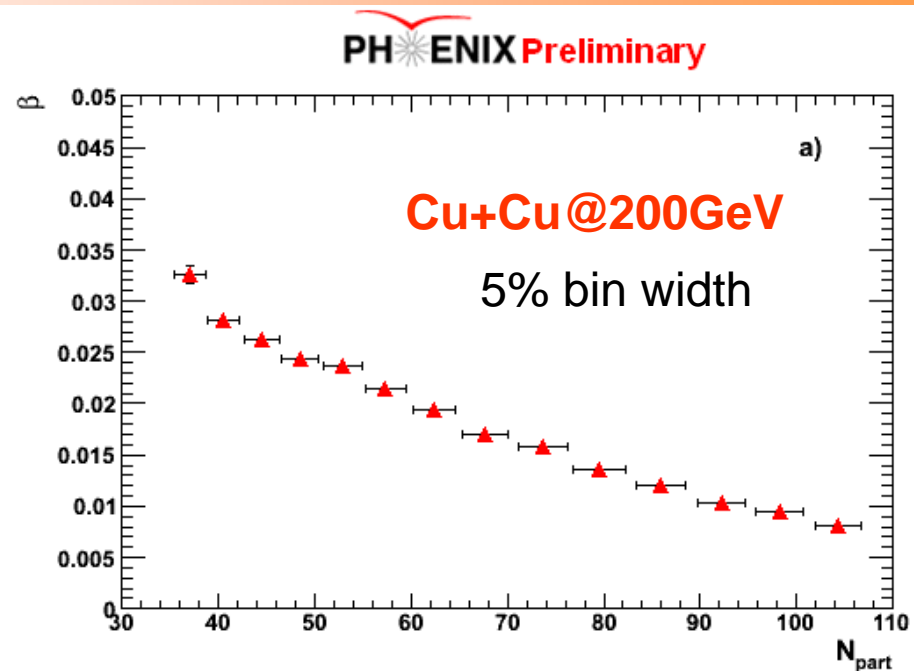
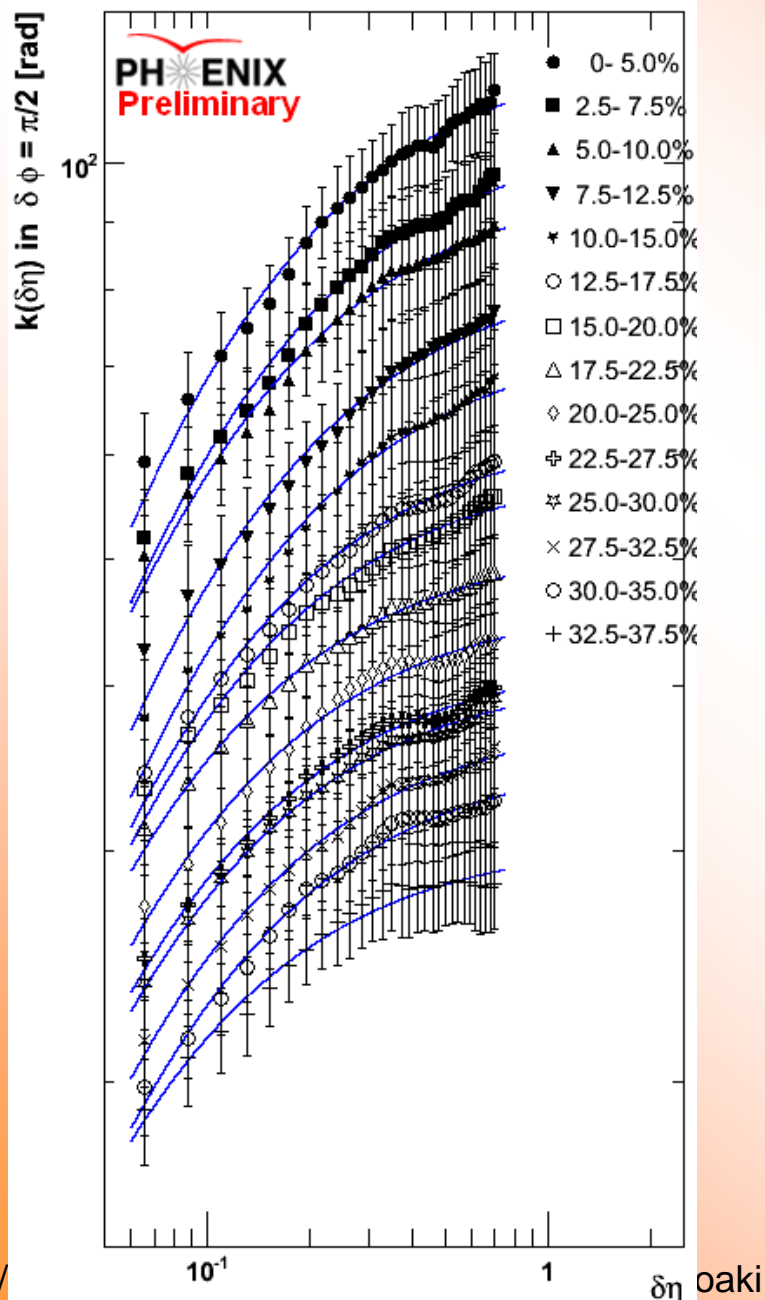
Cu+Cu@200GeV
5% bin width



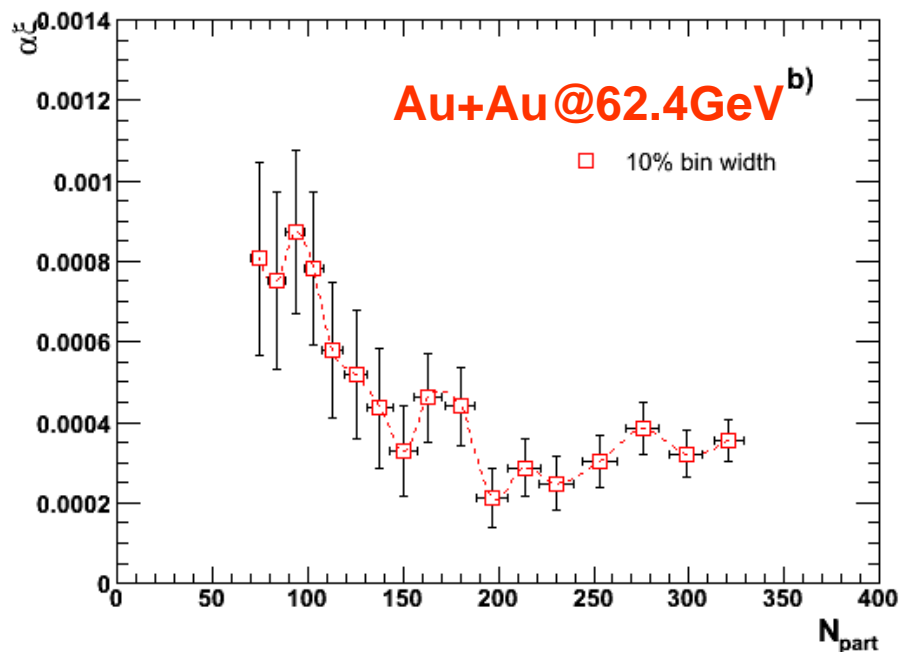
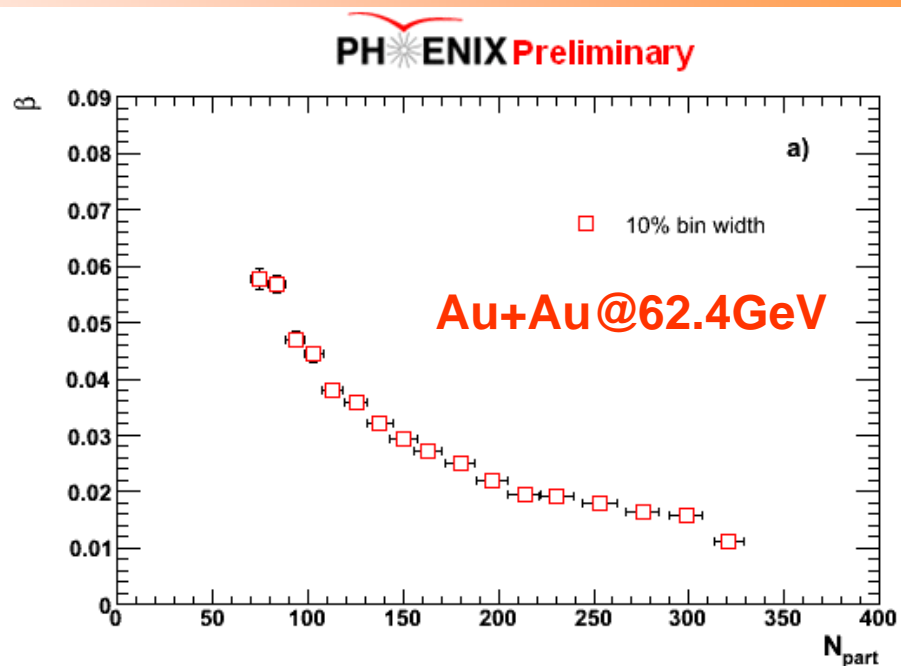
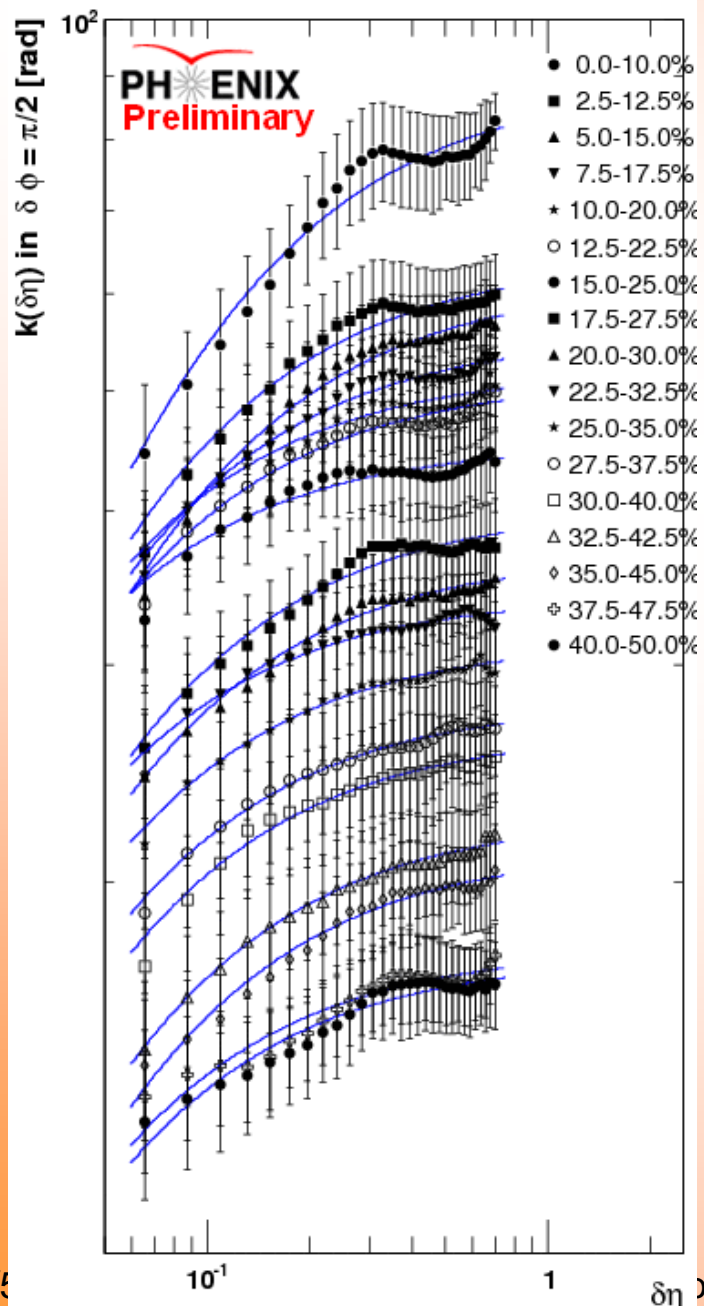
Au+Au@62.4GeV
10% bin width



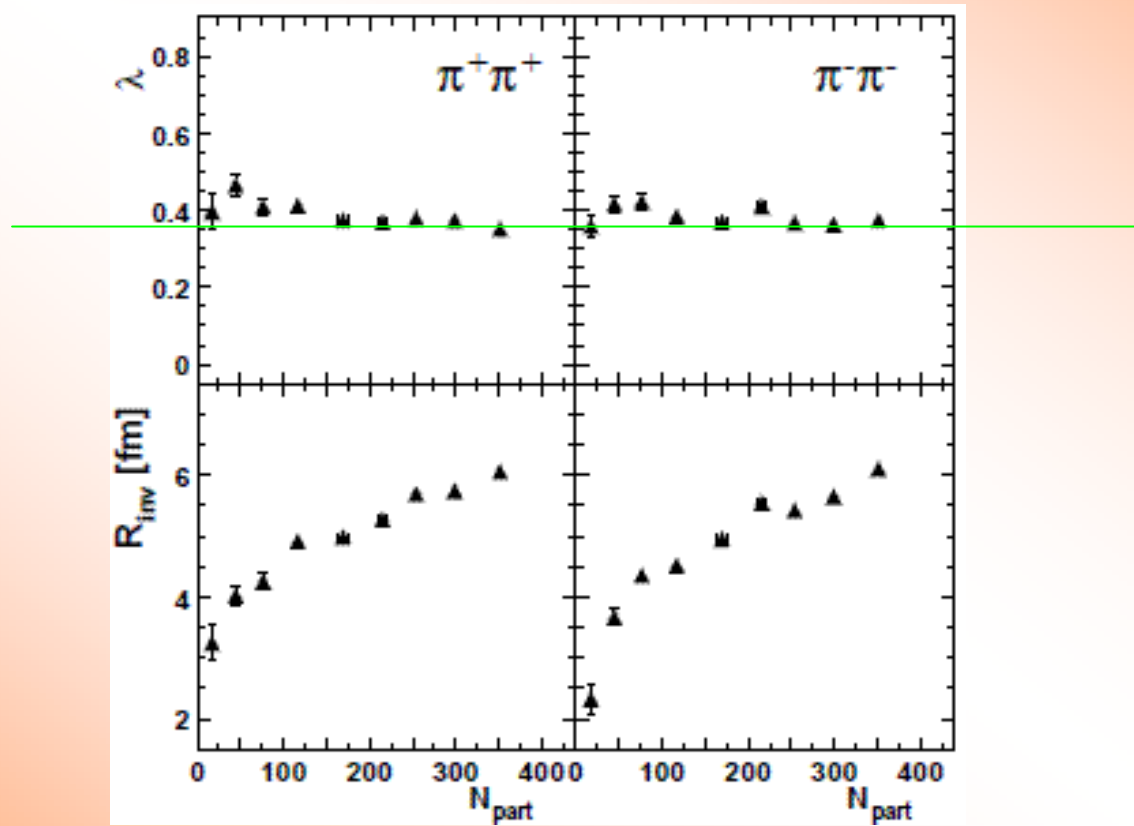
Analysis in smaller system: Cu+Cu@200GeV



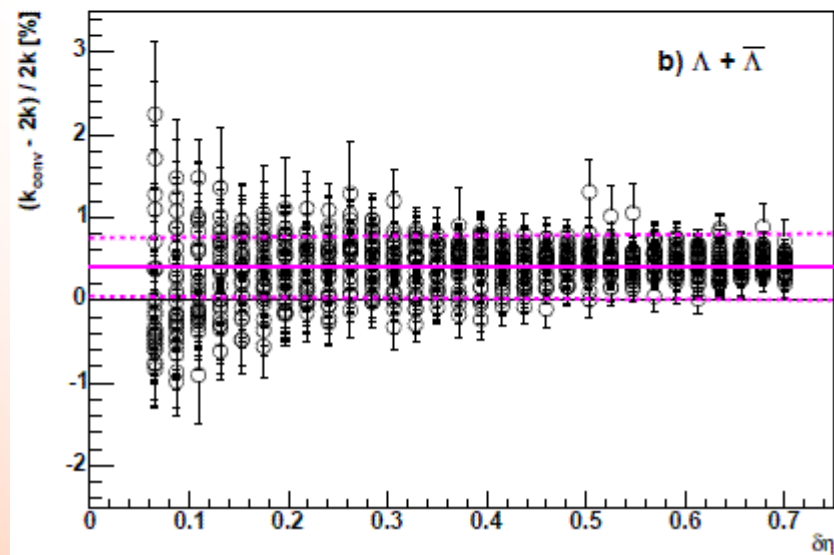
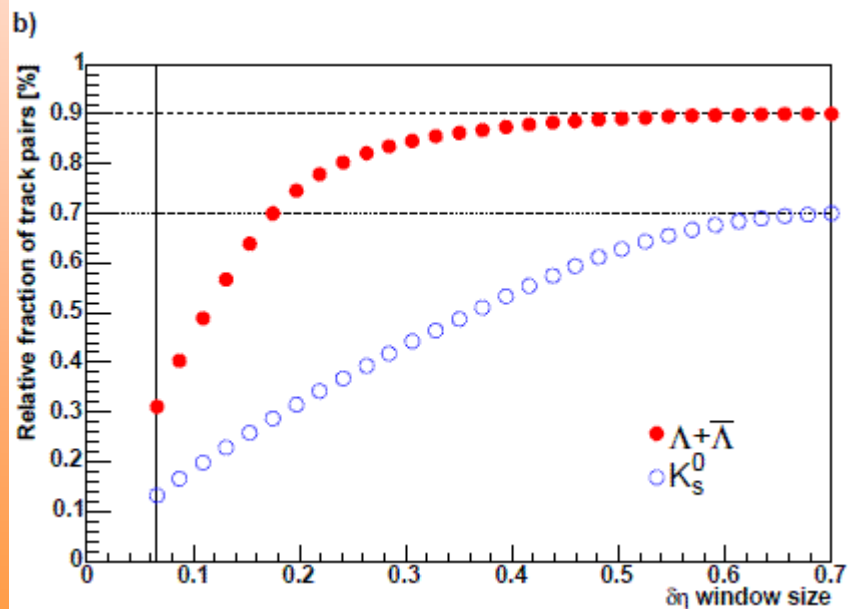
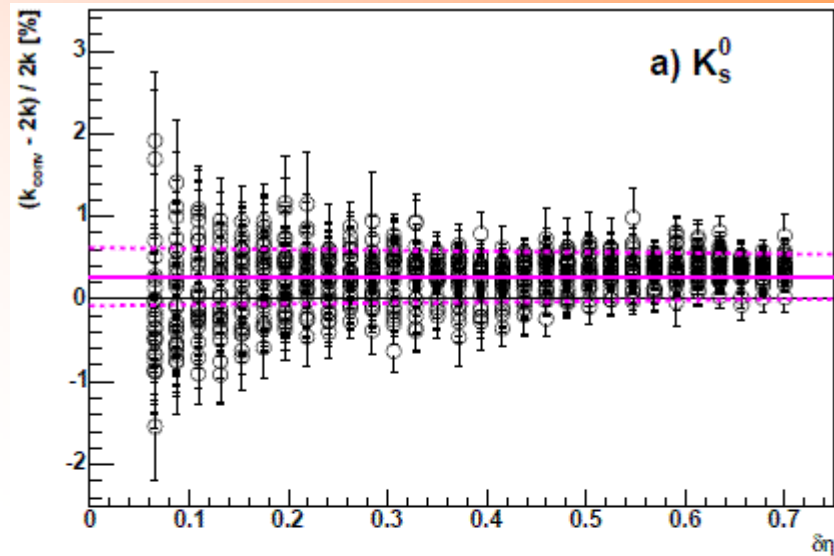
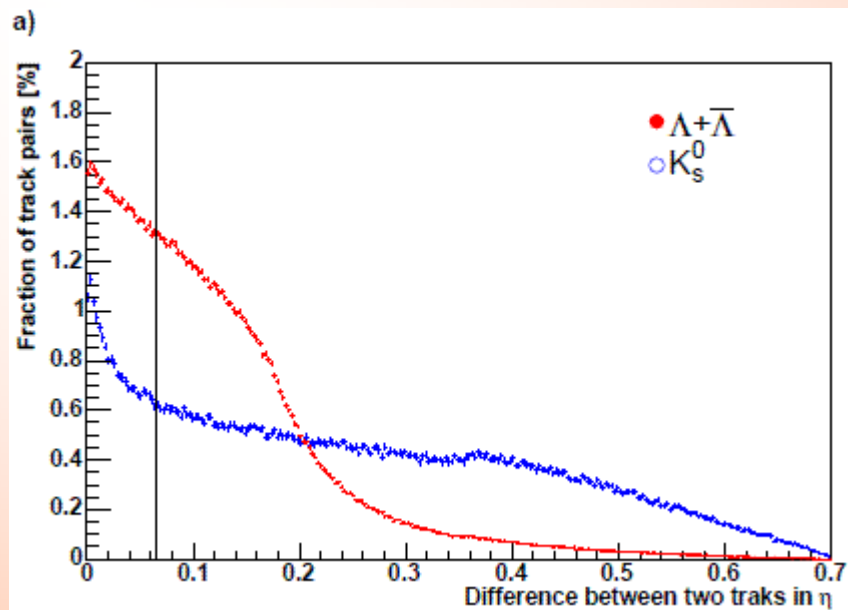
Analysis in lower energy: Au+Au@62.4GeV



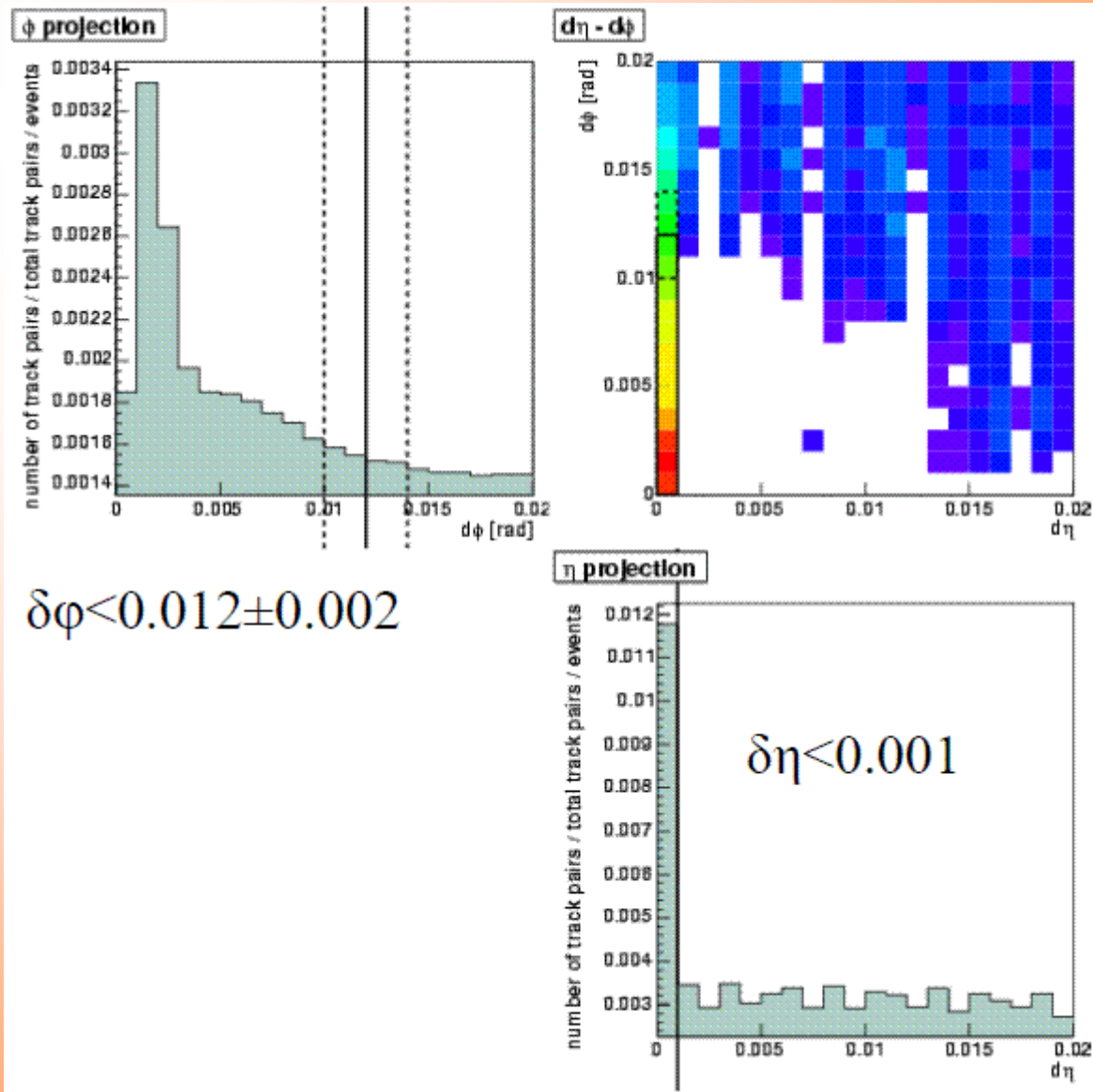
Trivial correlations (HBT)



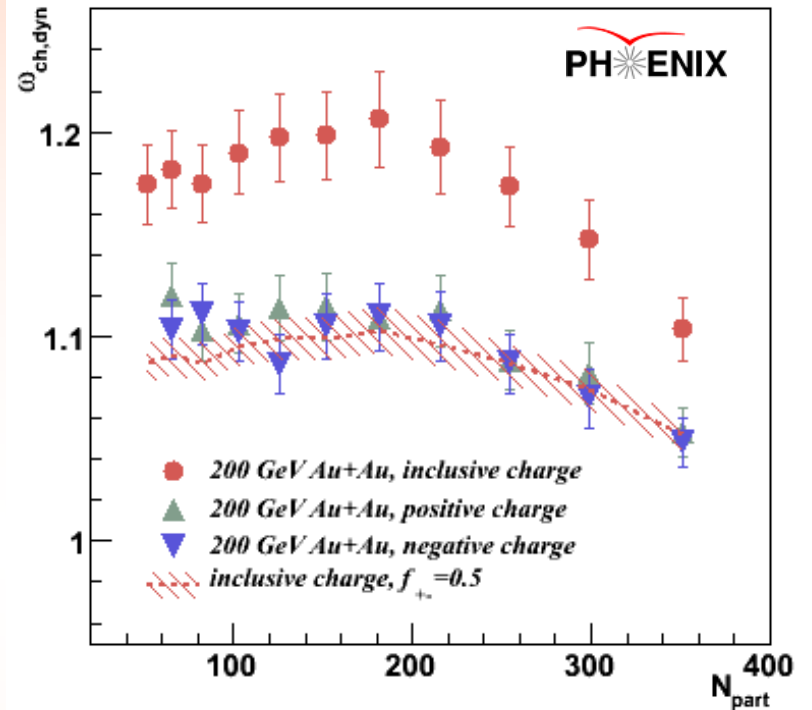
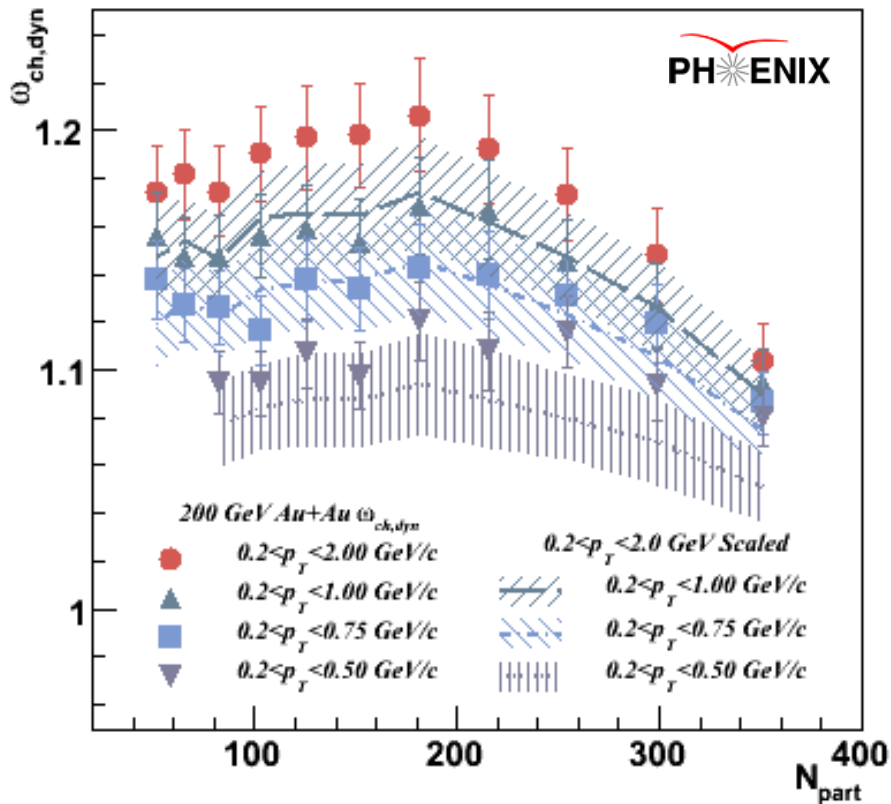
Trivial correlations (weak decays)



Trivial correlations (ghost & $\gamma \rightarrow ee$)



p_T and Charge Dependence



If the p_T -dependence is random, the scaled variance should scale with $\langle N \rangle$ in the same manner as acceptance:

$$\omega_{pT} = 1 - f + f\omega_{pT,max}$$

As with acceptance, with no charge-dependent correlation, the scaled variance will scale:

$$\omega_{+-} = 1 - f + f\omega_{inclusive}$$

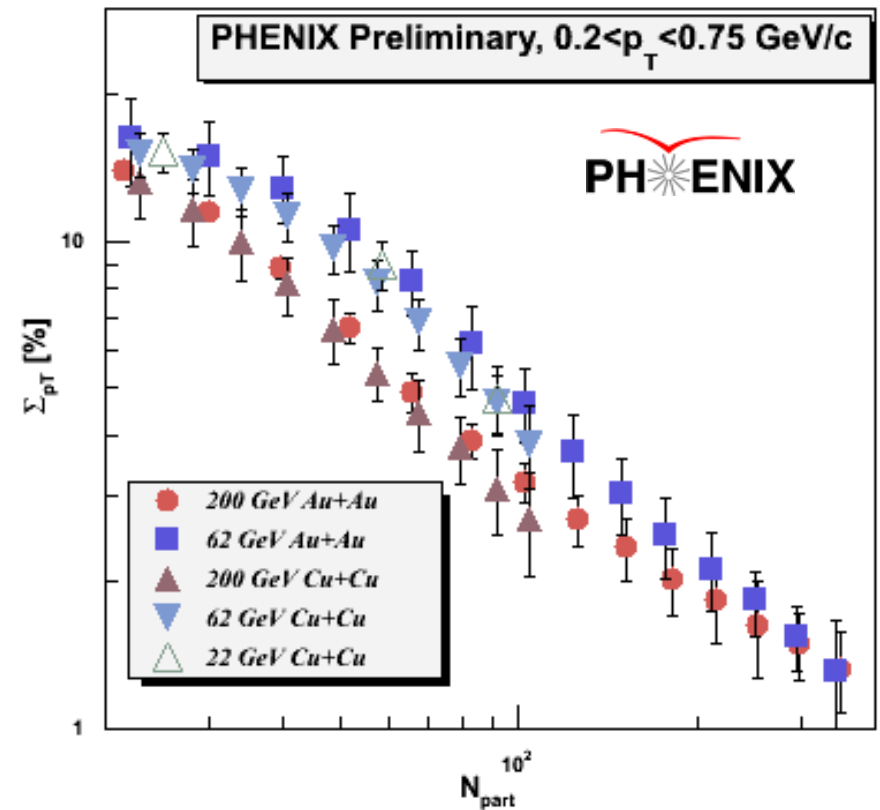
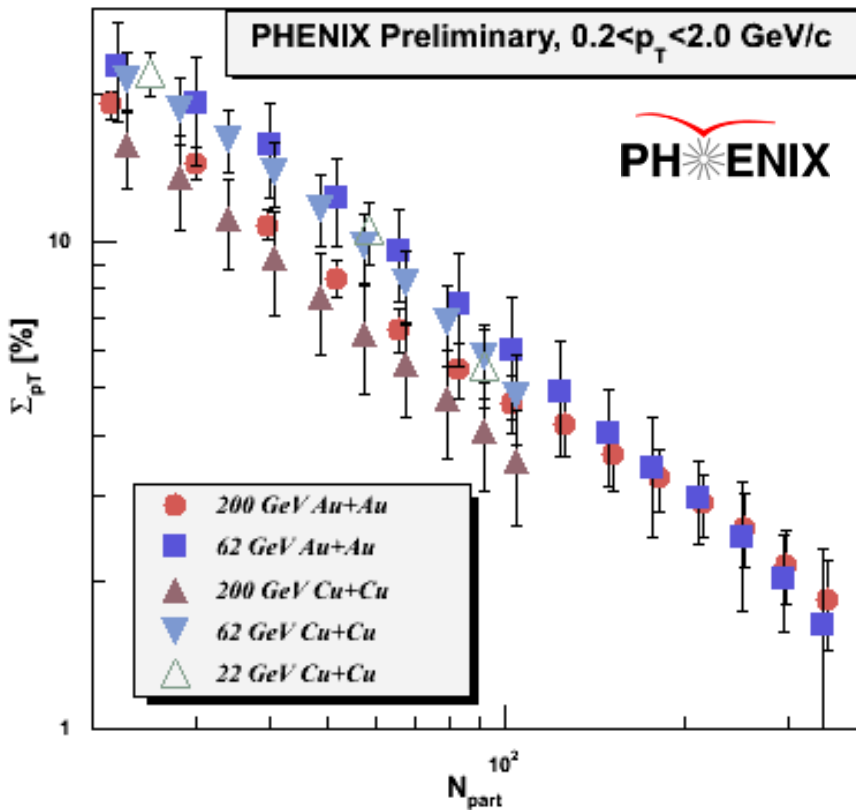
where $f=0.5$.

Within errors, no charge dependence of the fluctuations is seen for 200 GeV Au+Au.

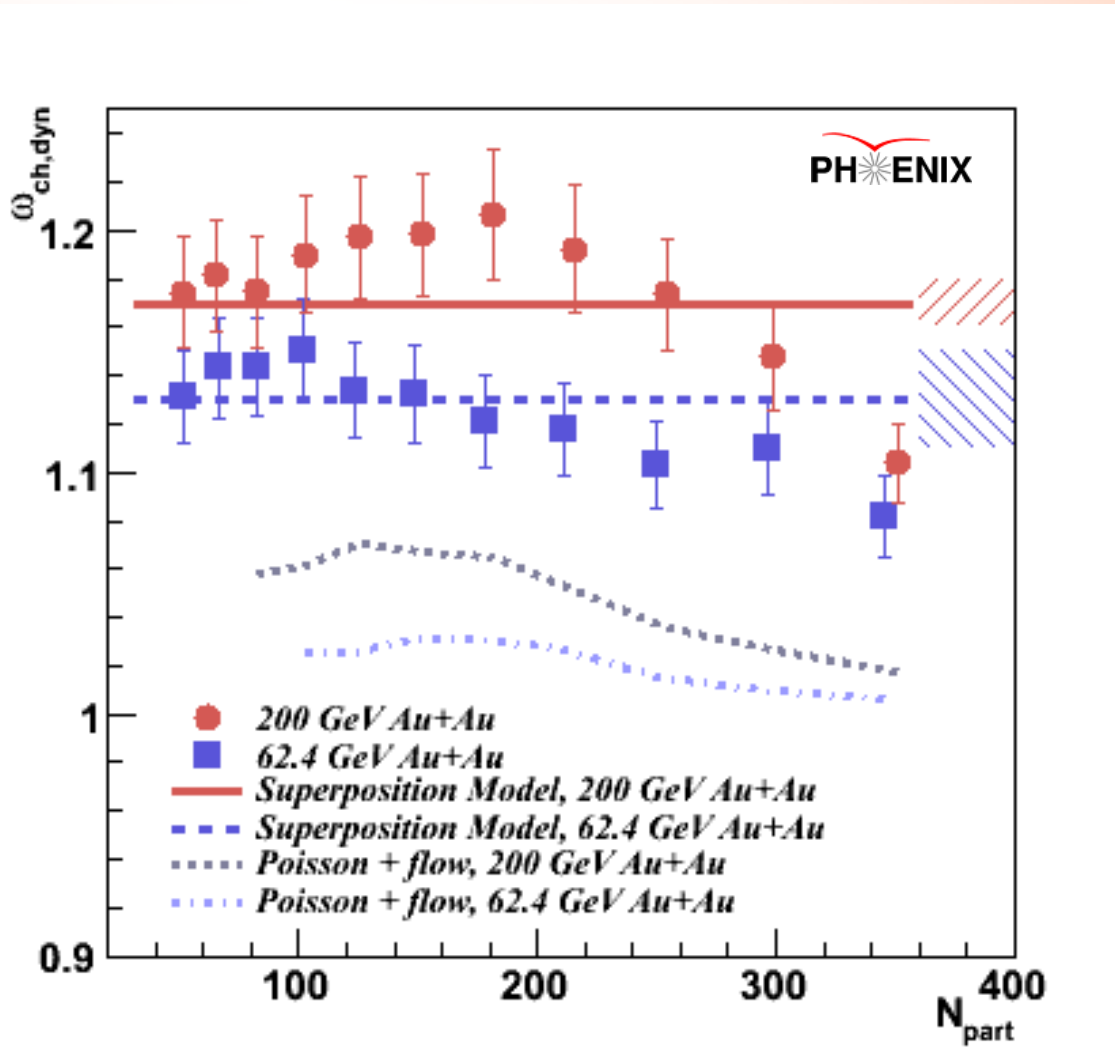
$\langle p_T \rangle$ Fluctuations vs. Centrality

Above $N_{part} \sim 30$, the data can be described by a power law in N_{part} , independent of the p_T range down to $0.2 < p_T < 0.5$ GeV/c:

$$\Sigma_{p_T} \propto N_{part}^{-1.02 \pm 0.10}$$



Multiplicity Fluctuations: Elliptic Flow



- The elliptic flow contribution estimated using a simple model as follows:
- For each event, a random reaction plane angle is generated.
- A particle azimuthal distribution is sampled using the PHENIX measured values of v_2 at the mean p_T of each bin.
- The multiplicity within the PHENIX acceptance is recorded for each event and the fluctuations are determined.
- The resulting contributions can be as large as 20% and can explain the centrality-dependence of the fluctuations.